Contribution of seasonal sub-Antarctic surface water variability to millennial-scale changes in atmospheric CO2 over the last deglaciation and Marine Isotope Stage 3

Julia Gottschalk, Luke C. Skinner, Claire Waelbroeck

Earth and Planetary Science Letters 411 (2015) 87–99

Contents lists available at ScienceDirect

Earth and Planetary Science Letters

www.elsevier.com/locate/epsl

Contribution of seasonal sub-Antarctic surface water variability to millennial-scale changes in atmospheric CO_2 over the last deglaciation and Marine Isotope Stage 3

Julia Gottschalk [a,*], Luke C. Skinner [a], Claire Waelbroeck [b]

[a] Godwin Laboratory for Palaeoclimate Research, Department of Earth Sciences, University of Cambridge, Cambridge CB2 3EQ, UK
[b] LSCE/IPSL Laboratoire, CNRS–CEA–UVSQ, 91198 Gif-sur-Yvette, France

ARTICLE INFO

Article history:
Received 19 July 2014
Received in revised form 25 November 2014
Accepted 29 November 2014
Available online 17 December 2014
Editor: J. Lynch-Stieglitz

Keywords:
South Atlantic
planktonic foraminifera
stable oxygen and carbon isotopes
atmospheric CO_2
last glacial period

ABSTRACT

The Southern Ocean is thought to have played a key role in past atmospheric carbon dioxide ($CO_{2,atm}$) changes. Three main factors are understood to control the Southern Ocean's influence on $CO_{2,atm}$, via their impact on surface ocean pCO_2 and therefore regional ocean–atmosphere CO_2 fluxes: 1) the efficiency of air–sea gas exchange, which may be attenuated by seasonal- or annual sea-ice coverage or the development of a shallow pycnocline; 2) the supply of CO_2-rich water masses from the sub-surface and the deep ocean, which is associated with turbulent mixing and surface buoyancy- and/or wind forcing; and 3) biological carbon fixation, which depends on nutrient availability and is therefore influenced by dust deposition and/or upwelling. In order to investigate the possible contributions of these processes to millennial-scale $CO_{2,atm}$ variations during the last glacial and deglacial periods, we make use of planktonic foraminifer census counts and stable oxygen- and carbon isotope measurements in the planktonic foraminifera *Globigerina bulloides* and *Neogloboquadrina pachyderma* (sinistral) from marine sediment core MD07-3076Q in the sub-Antarctic Atlantic. These data are interpreted on the basis of a comparison of core-top and modern seawater isotope data, which permits an assessment of the seasonal biases and geochemical controls on the stable isotopic compositions of *G. bulloides* and *N. pachyderma* (s.). Based on a comparison of our down-core results with similar data from the Southeast Atlantic (Cape Basin) we infer past basin-wide changes in the surface hydrography of the sub-Antarctic Atlantic. We find that millennial-scale rises in $CO_{2,atm}$ over the last 70 ka are consistently linked with evidence for increased spring upwelling, and enhanced summer air–sea exchange in the sub-Antarctic Atlantic. Parallel evidence for increased summer export production would suggest that seasonal changes in upwelling and air–sea exchange exerted a dominant influence on surface pCO_2 in the sub-Antarctic Atlantic. These results underline the role of Southern Ocean dynamics, in particular their seasonal variations, in driving millennial-scale variations in $CO_{2,atm}$.

1. Introduction

The ocean is a large and dynamic carbon reservoir that is tightly connected to the atmosphere via the solubility and reactivity of CO_2 in seawater (Sigman and Boyle, 2000). It has long been thought that the high-latitude oceans, in particular the Southern Ocean, may exert a dominant influence on ocean–atmosphere carbon exchange (e.g. Sarmiento and Toggweiler, 1984; Siegenthaler and Wenk, 1984). This dominance stems from the connection between the large deep-ocean carbon pool and the atmosphere, which is promoted by an exchange between the surface Southern Ocean and the sub-surface/deep ocean provided by outcropping isopycnals (constant density surfaces). The exchange between the surface and deep oceans in the southern high-latitudes is controlled by turbulent mixing in the ocean interior and the Southern Ocean residual overturning circulation (Marshall and Speer, 2012), which are driven respectively by internal energy dissipation (Wunsch and Ferrari, 2004) and surface wind- and buoyancy forcing (Toggweiler et al., 2006; Watson and Naveira Garabato, 2006). This particular setting makes the Southern Ocean the region, where most water in the ocean interior first makes contact

* Corresponding author. Tel.: +44 (0) 1223 768342.
E-mail address: jg619@cam.ac.uk (J. Gottschalk).

http://dx.doi.org/10.1016/j.epsl.2014.11.051

with the sea surface (i.e. upwells), and where most water also last makes contact with the sea surface (i.e. is exported from) (Gebbie and Huybers, 2011). The Southern Ocean is therefore the deep-ocean's main 'window' on the atmosphere.

The Southern Ocean is currently a High-Nutrient-Low-Chlorophyll region, where the total nutrient pool remains underutilized, and where export productivity does not, on average, keep pace with the upwelling of high-pCO_2 deep-waters (Sigman et al., 2010). For these reasons, it has been proposed that the Southern Ocean has played a central role in past (glacial–interglacial and millennial-scale) $CO_{2,atm}$ variations, whether via changes in air–sea exchange, buoyancy forcing and mixing in the upper water column (e.g. Stephens and Keeling, 2000; Watson and Naveira Garabato, 2006), wind-driven upwelling (Anderson et al., 2009; Toggweiler et al., 2006), or iron-fertilization driven export productivity (Martínez-García et al., 2014).

Today, upwelling in the southern high-latitude ocean dominates the austral winter season, whereas biological sequestration of carbon prevails in austral summer (Takahashi et al., 2002). The oceanic role in variations in $CO_{2,atm}$ is linked to the balance between these two processes (Metzl et al., 1999; Takahashi et al., 2002) and varies spatially in the southern high-latitude ocean (Marinov et al., 2006). A strong evasion of CO_2 dominates Antarctic waters south of the Polar Front (PF), whereas strong export production in the sub-Antarctic Zone (SAZ) north of the PF sequesters carbon (Marinov et al., 2006). The location of the divide between these regions might have been affected by shifts of the Southern Ocean frontal system, which has been shown to amount to ~5° change in latitude over glacial–interglacial transitions (Gersonde et al., 2003; Kohfeld et al., 2013). These frontal shifts can be tracked by changes in planktonic foraminifer assemblages in the surface ocean (Barker et al., 2009; Weaver et al., 1998). However, a paucity of well-resolved and well-dated marine records that bear on the seasonal differentiation of upwelling, air–sea gas exchange and export productivity has so far hampered our understanding of how these factors may have contributed to past changes in the surface ocean pCO_2 and thus $CO_{2,atm}$, in particular on millennial timescales.

The stable oxygen and carbon isotope composition of stenotopic planktonic foraminifera has previously been used for reconstructing seasonal variations in hydrography and stratification of the upper water column. The difference between $\delta^{18}O$ ($\Delta\delta^{18}O$) of co-existing surface- and deep-dwelling foraminifera has been linked to the temperature and salinity structure of the water column (Mortyn et al., 2002; Mulitza et al., 1997; Niebler et al., 1999). Similarly, the $\Delta\delta^{18}O$ of planktonic foraminifera calcifying in the same water depth but different seasons may relate to seasonal temperature and water-$\delta^{18}O$ variability at that water depth (Peeters et al., 2002; Williams et al., 1981).

Planktonic $\delta^{13}C$ reflects the $\delta^{13}C$ of dissolved inorganic carbon (DIC) in the ambient water in which the foraminifer calcifies (Spero, 1992), with possible additional impacts of temperature, carbonate ion (CO_3^{2-}) concentration, photosynthetic symbiont activity or changes in the isotopic composition of the foraminifer's diet for example (e.g. Bemis et al., 2000; Spero and Lea, 1996). Winter upwelling in the Southern Ocean supplies additional respired nutrients and therefore acts to deplete the $\delta^{13}C$ of DIC ($\delta^{13}DIC$) in the surface ocean. In contrast, photosynthesis during summer utilizes isotopically light DIC and thus enriches the $\delta^{13}DIC$ of surface waters. Abiotic effects, e.g. the air–sea exchange of CO_2, additionally influence surface water $\delta^{13}DIC$ (Lynch-Stieglitz et al., 1995). If these influences are taken into account, or are invariant, nutrient gradients in the upper water column can in principle be derived from the $\delta^{13}C$ difference ($\Delta\delta^{13}C$) between coexisting surface- and deep-dwelling foraminifera (Mulitza et al., 1998). Similarly, seasonal changes in $\delta^{13}DIC$ can be inferred from planktonic foraminifera with different calcifying seasons but a similar depth habitat (Jonkers et al., 2013).

Here, we present centennially resolved stable isotope records of *G. bulloides* and *N. pachyderma* (s.) from marine sediment core MD07-3076Q (44°9.2′S, 14°13.7′W, 3770 m water depth) from the sub-Antarctic Atlantic in order to assess possible links between seasonally differentiated changes in upwelling, air–sea exchange and export productivity and millennial-scale changes in $CO_{2,atm}$ during the last glacial and deglacial periods. We interpret these changes in the light of variations in the position of the fronts inferred from planktonic foraminifer census counts. Moreover, we test our assumptions on habitat depth and calcifying season of both planktonic foraminifera based on a meridional transect of compiled core-top stable oxygen and carbon isotopes in the South Atlantic before applying them to the down-core record. A synthesis of all available, high-resolution CO_2 records transferred to the newly established AICC2012 age scale (Veres et al., 2013) allows a direct comparison of hydrographic changes in the surface ocean with changes in $CO_{2,atm}$.

2. Study area

2.1. Regional hydrography

Marine sediment core MD07-3076Q has been retrieved from the eastern flank of the mid-Atlantic ridge (Fig. 1a). It is located within the modern SAZ, which is confined by the sub-Tropical Front (STF) to the north and by the sub-Antarctic Front (SAF) to the south (Fig. 1a). The STF coincides with the 10–12 °C-isotherms at 100 m depth, whereas the position of the SAF is described as the northern boundary of the low-salinity tongue of Antarctic Intermediate Water (AAIW) in surface waters (Orsi et al., 1995). The SAZ is defined by a distinct sub-surface salinity minimum associated with the formation of AAIW further to the south (Orsi et al., 1995). The PF further to the south (Fig. 1a) coincides with a sub-surface temperature minimum of about 2 °C (Belkin and Gordon, 1996). South of the PF, wind-driven Ekman transport leads to the upwelling of CO_2- and nutrient-rich water masses in the Antarctic Divergence Zone, which coincides with the southern limit of the Antarctic Circumpolar Current (Orsi et al., 1995).

2.2. Modern planktonic foraminifer assemblages

At present-day, the cold-water species *N. pachyderma* (s.) dominates the region south of the SAF (Fig. 1; Bé, 1969; Hemleben et al., 1989; Kohfeld et al., 1996). The highest abundance of *Turborotalita quinqueloba* coincides with the abundance maximum of *N. pachyderma* (s.) (Fig. 1; Bé, 1969; Niebler and Gersonde, 1998). *G. bulloides* is very abundant in the SAZ (Fig. 1) and is indicative of cold and nutrient-rich water masses of upwelling regions (Fig. 1; e.g. Bé, 1969; Peeters et al., 2002). High abundances of *N. pachyderma* dextral (d.) occur in upwelling regions and north of the STF (Fig. 1). *Globigerina inflata* shows a wide distribution from the sub-Tropical to the Antarctic Zones (Fig. 1; Niebler et al., 1999) and is characteristic for the transitional zone between sub-Antarctic and sub-Tropical waters (Bé, 1969). *Globorotalia truncatulinoides* and *Globigerina falconensis* both thrive in sub-Tropical waters (Fig. 1; Bé, 1969; Niebler et al., 1999). The latter prefers the cooler edges of the sub-Tropical Zone (Bé, 1969).

2.3. Calcifying season and depth habitat of G. bulloides and N. pachyderma (s.)

Based on sediment trap analyses south of Tasmania, *G. bulloides* and *N. pachyderma* (s.) have been shown to thrive in a near-surface

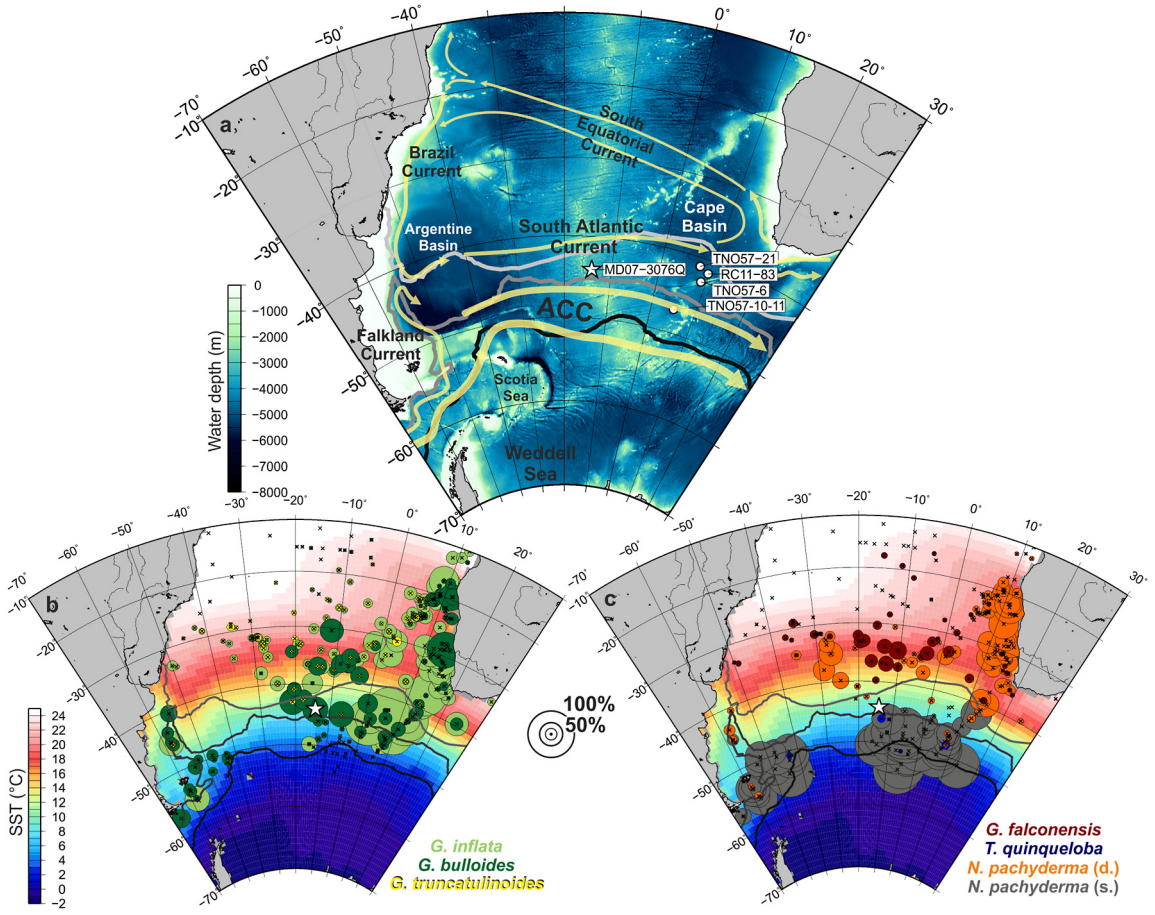

Fig. 1. Surface water hydrography and planktonic foraminifer assemblages in the South Atlantic and the Atlantic Sector of the Southern Ocean: a) surface ocean currents (Peterson and Stramma, 1991; Stramma and England, 1999) and the position of major fronts (from south to north: Polar Front (dark grey line), sub-Antarctic Front (grey line), sub-Tropical Front (light grey line); Orsi et al., 1995; Sokolov and Rintoul, 2009), and b), c) mean annual sea surface temperature (SST) from the World Ocean Atlas 2009 (Locarnini et al., 2010) with the position of fronts and the sediment core-top abundance of *N. pachyderma* (s.) (grey), *T. quinqueloba* (dark blue), *G. bulloides* (dark green), *G. inflata* (light green), *G. falconensis* (dark red), *G. truncatulinoides* (yellow) and *N. pachyderma* (d.) (orange) (circle size indicates the fraction (%) of individual planktonics to the whole planktonic assemblage at the location; Kucera et al., 2005; Niebler, 1995); the white star and circles mark the location of the study core and further sediment cores mentioned in the text, respectively. (For interpretation of the references to color in this figure legend, the reader is referred to the web version of this article.)

habitat in the SAZ (King and Howard, 2005), which is consistent with observations in the Atlantic Ocean (Deuser and Ross, 1989; Jonkers et al., 2013; Niebler et al., 1999). In the southern PF Zone, *N. pachyderma* (s.) dwells slightly deeper than *G. bulloides* (King and Howard, 2005). High abundances of *G. bulloides* have been found at depths of fluorescence peaks and maximum chlorophyll concentrations (Mortyn and Charles, 2003), which suggests an association of *G. bulloides* with phytoplankton blooms and an enhanced availability of food. An increase in the abundance of *G. bulloides* in the SAZ primarily occurs during spring, which is linked to a decrease of the mixed layer depth (MLD) and the associated shoaling of the chlorophyll maximum (King and Howard, 2003). In contrast, *N. pachyderma* (s.) has been shown to calcify in the SAZ mostly during summer, which reflects its preference for very shallow MLDs and high surface chlorophyll concentrations that occur during intense summer density stratification of the water column (King and Howard, 2003, 2005). The modern MLD (World Ocean Atlas (WOA) 2009; Locarnini et al., 2010) in the SAZ decreases from 250 m in austral winter to 70 m during austral summer. The season of maximum fluxes of *G. bulloides* shifts from spring in the SAZ to late spring and summer in the southern PF Zone (King and Howard, 2003, 2005). The flux of *N. pachyderma* (s.) remains strongest during austral summer in the southern PF Zone and south of the PF (Donner and Wefer, 1994; King and Howard, 2003, 2005).

3. Methods

3.1. Stable isotopes

Stable isotopic analyses on *G. bulloides* and *N. pachyderma* (s.) have been performed on 30 and 40 individuals from the 250–300 µm and 212–250 µm size fractions, respectively. The samples were measured on Finnigan Δ+ and Elementar Isoprime mass spectrometers at the LSCE in Gif-sur-Yvette (France). Oxygen and carbon isotopic shell composition is expressed as deviation from the NBS-19 calcite standard (Coplen, 1988) as $\delta^{18}O$ and $\delta^{13}C$ in ‰ versus Vienna Pee Dee Belemnite (PDB), respectively. The mean external reproducibility of carbonate standards is $\sigma \pm 0.05$‰ for $\delta^{18}O$ and $\sigma \pm 0.03$‰ for $\delta^{13}C$. The isotope data are available from the Pangaea database.

The compilation of the planktonic $\delta^{18}O$ and $\delta^{13}C$ data is based on published (Duplessy et al., 1991; Keigwin and Boyle, 1989; Kohfeld et al., 2000; Mulitza et al., 1997; Niebler, 1995; Niebler et al., 1999) and unpublished data (Hubberten and Niebler, pers. comm.; Table S1), and is described in more detail in the supporting online material (SOM).

3.2. Census counts

Planktonic foraminifera were counted from a sample aliquot of the size fraction >150 µm to a total number of >300 (CLIMAP project members, 1984). Planktonic foraminiferal assemblages are

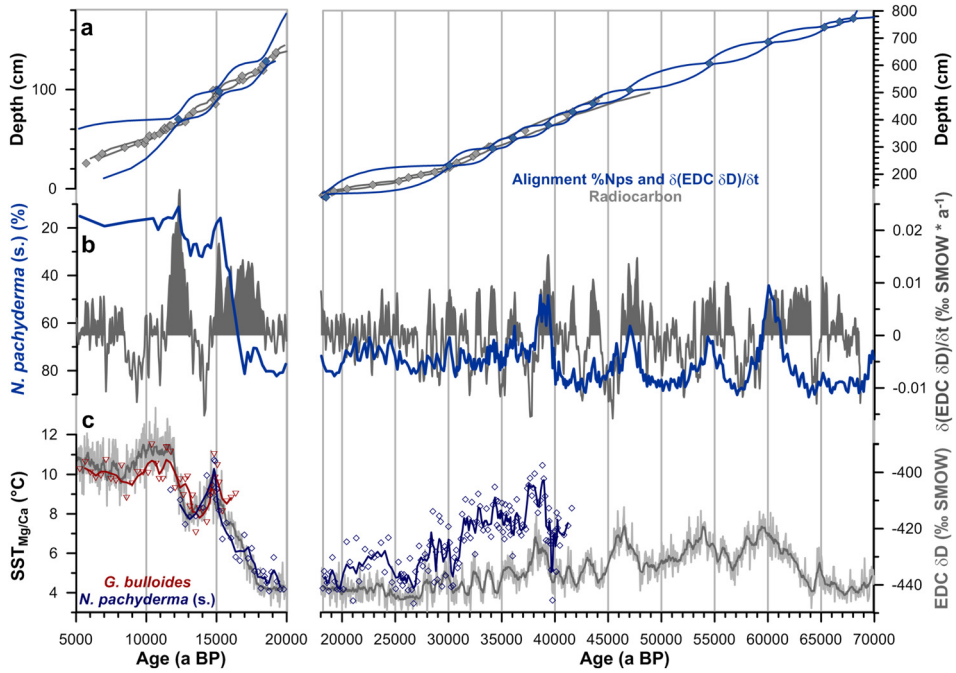

Fig. 2. Age model details for the last deglaciation (left) and the last glacial period (right) recorded in MD07-3076Q: a) depth-age tiepoints derived from radiocarbon measurements (grey) (Skinner et al., 2010) and the stratigraphic alignment of the abundance peaks of *N. pachyderma* (s.) (%Nps) with the first derivative of the EPICA Dome C (EDC) δD record (Jouzel et al., 2007) on the AICC2012 age scale (Veres et al., 2013) performed in this study (dark blue), envelopes show the associated age model uncertainties (95% highest posterior density region) calculated with the Bayesian statistical software BCHRON (Haslett and Parnell, 2008); b) changes in the abundance of *N. pachyderma* (s.) (dark blue) and the rate of change of EDC δD (grey; detrended and smoothed by a 200 years window) shown on the *N. pachyderma* (s.) abundance-based chronology; c) correlation of EDC δD (grey) and Mg/Ca-sea surface temperature (SST) (Skinner et al., 2010) obtained from *G. bulloides* (dark red) and *N. pachyderma* (s.) (dark blue) based on the final age model (solid lines represent 3-point running averages). (For interpretation of the references to color in this figure legend, the reader is referred to the web version of this article.)

expressed as the number of the individual planktonic species with respect to the total number of whole planktonics in percent. The data are stored in the Pangaea database. The uncertainty (1σ) of determined planktonic foraminifer abundances has been inferred from 15 replicate counts and amounts to 1.4%. We categorize the different planktonic species as Antarctic (*N. pachyderma* (s.), *T. quinqueloba*), sub-Antarctic (*G. bulloides*), transitional (*G. inflata*) and sub-Tropical (*G. truncatulinoides*, *N. pachyderma* (d.), *G. falconensis*).

3.3. Chronologies

3.3.1. Sediment core MD07-3076Q

Chronological control of MD07-3076Q is based on radiocarbon measurements and the stratigraphic alignment of sea surface temperature (SST) proxies with Antarctic temperature. The radiocarbon-dated sediment section of MD07-3076Q is based on a calibration of 59 radiocarbon dates with the IntCal04 and Cariaco datasets (Hughen et al., 2006; Reimer et al., 2004) using variable reservoir ages corrections (Skinner et al., 2010). It has been shown that a calibration with a different atmospheric reference dataset (and accordingly revised reservoir age corrections) makes a negligible difference to the chronology (Skinner et al., 2014). The radiocarbon ages have been transferred to calibrated calendar ages using the Bayesian statistical software package BCHRON (Haslett and Parnell, 2008).

Chronostratigraphic constraints can also be derived from the alignment of SST estimates in MD07-3076Q based on foraminiferal Mg/Ca ratios (Mashiotta et al., 1999; Nürnberg et al., 1996) or *N. pachyderma* (s.) abundances (Govin et al., 2009) with the Antarctic temperature proxy δD in the EPICA Dome C (EDC) ice core. Mg/Ca-derived SSTs have been shown to closely match Antarctic temperatures as shown by their representation of a gradual warming of the southern high-latitudes in synchrony with inter-hemispheric heat transport associated with the bipolar seesaw (Barker et al., 2009). In contrast, rapid changes in planktonic foraminifer assemblages have been suggested to relate to rapid adjustments of the oceanic fronts during Antarctic warming periods rather than to temperature changes of the ambient water masses alone (Barker et al., 2009). We therefore align minima in the abundance of *N. pachyderma* (s.) in MD07-3076Q to warming phases over Antarctica, i.e. maxima of the first derivative of the EDC δD record (Fig. 2), applying the AICC2012 chronology (Veres et al., 2013). The resulting age model produces an excellent match between Mg/Ca SSTs and the EDC δD temperature proxy (Fig. 2), consistent with the expectations outlined above.

Where they overlap, the *N. pachyderma* (s.) abundance-based chronology and the radiocarbon-based age model are in excellent agreement (Fig. 2). They deviate from each other by 500 ± 400 years on average, which is within uncertainties of the age models (Fig. S1). This lends credibility to the applied stratigraphic alignment during MIS 3, beyond the limit of radiocarbon dating.

Prior to 27 ka BP, a lack of reservoir age constraints and increasing uncertainties of the atmospheric calibration curves result in relatively large uncertainties of the radiocarbon-based chronology (Skinner et al., 2010). We therefore use the radiocarbon age model for the upper core section (<27 ka BP) and rely on the age-depth markers resulting from the alignment of *N. pachyderma* (s.) with the rate of change in Antarctic temperature for the older core section (>27 ka BP) (Fig. 2, Table S2).

Absolute chronological uncertainties amount to about 1200 ± 400 years for the period between 27 and 10 ka BP (Skinner et al., 2010). Mean age uncertainties of the *N. pachyderma* (s.)-based chronology between 68 and 27 ka BP strongly depend on the tie-point density and amount to about 1600 ± 500 years (Fig. S1).

3.3.2. Gas age scales of CO_2 records from Antarctic ice cores

In order to facilitate comparisons of our marine data with records of $CO_{2,atm}$, we have compiled all of the available high-resolution ice core CO_2 data from the last deglacial and glacial periods (Fig. S2) and placed them on the AICC2012 age scale (Veres et al., 2013) as described in the SOM.

4. Results

4.1. Comparison between South Atlantic core-top $\delta^{18}O$ and $\delta^{13}C$ of G. bulloides and N. pachyderma (s.) and the modern hydrography

Closely matching core-top $\delta^{18}O$ values of *G. bulloides* and *N. pachyderma* (s.) north of the PF parallel predicted calcite $\delta^{18}O$ ($\delta^{18}O_{pred}$) according to the species-specific palaeotemperature equations of Bemis et al. (1998) (13-chambered *G. bulloides*) and Mulitza et al. (2003) (*N. pachyderma* s.) (Fig. 3). Planktonic $\delta^{18}O_{pred}$ has been calculated based on seawater-$\delta^{18}O$ after Schmidt et al. (1999) and seasonal SST extracted from WOA 2009 (Locarnini et al., 2010). The relative constant offset of planktonic $\delta^{18}O$ from near-surface water $\delta^{18}O_{pred}$ north of the PF may be explained by gametogenic encrustation (Kohfeld et al., 1996; Kozdon et al., 2009), the CO_3^{2-} effect (Spero et al., 1997) and/or other disequilibrium effects, which are not considered by the species-specific palaeotemperature equations (Bemis et al., 1998; Mulitza et al., 2003). The suggested change in depth habitat of *N. pachyderma* (s.) in the southern PF Zone south of Tasmania appears to be associated with the PF in the Atlantic Sector of the Southern Ocean, where a marked divergence of both planktonic $\delta^{18}O$ signatures in core-top sediments is observed (Fig. 3). Given the evidence of an overlapping depth habitat of *G. bulloides* and *N. pachyderma* (s.) north of the PF indicated by closely matching core-top $\delta^{18}O$ values (Fig. 3), the offset in $\delta^{13}C$ values of both planktonic species in core-top samples north of the PF suggests that *G. bulloides* and *N. pachyderma* (s.) calcify their test in different seasons, which has been observed south of Tasmania (King and Howard, 2003). In line with these data, we assume that north of the PF *G. bulloides* and *N. pachyderma* (s.) predominantly calcify during spring and summer, respectively.

Equilibrium $\delta^{13}C$ ($\delta^{13}C_{eq}$) of inorganically precipitated calcite is expected to be enriched by 1‰ relative to seawater $\delta^{13}DIC$ (Romanek et al., 1992). At present, the spatial and seasonal variability in surface water $\delta^{13}DIC$ in the Southern Ocean north of the PF is very small (Fig. 3), as biotic (photosynthesis, respiration) and abiotic processes (kinetic fractionation effects during the air–sea exchange of CO_2, temperature-dependent isotopic air–sea CO_2 equilibration) (Lynch-Stieglitz et al., 1995) cancel each other out (Gruber et al., 1999). However, south of the PF surface water $\delta^{13}DIC$ is lower in spring than in summer and autumn, indicative of the influence of upwelling of $\delta^{13}C$-depleted water masses during the spring (Fig. 3). The surface water $\delta^{13}DIC$ maximum seen in all seasons in the vicinity of the SAZ reflects enhanced air–sea exchange of CO_2 (Gruber et al., 1999), which is related to the maximum in zonal wind stress (Fig. 3).

Core-top carbon isotopes of *G. bulloides* and *N. pachyderma* (s.) in the South Atlantic disagree with calcite $\delta^{13}C_{eq}$ during the expected season and habitat of *G. bulloides* and *N. pachyderma* (s.) and are generally lighter by 1.5 to 2.5‰ (Fig. 3). It has been suggested that temperature (e.g. Bemis et al., 2000), CO_3^{2-} (Spero et al., 1997) and dietary effects (Spero and Lea, 1996) account for this observed $\delta^{13}C$ disequilibrium (Kohfeld et al., 2000). The effect of calcification temperature on the metabolic rates of shell calcification and carbon uptake amounts to a decrease of planktonic $\delta^{13}C$ by 0.13‰ per 1 °C warming (Bemis et al., 2000; Spero and Lea, 1996). The CO_3^{2-} concentration in the surface ocean has been suggested to be related with the pH-dependent bioavailability of ^{12}C

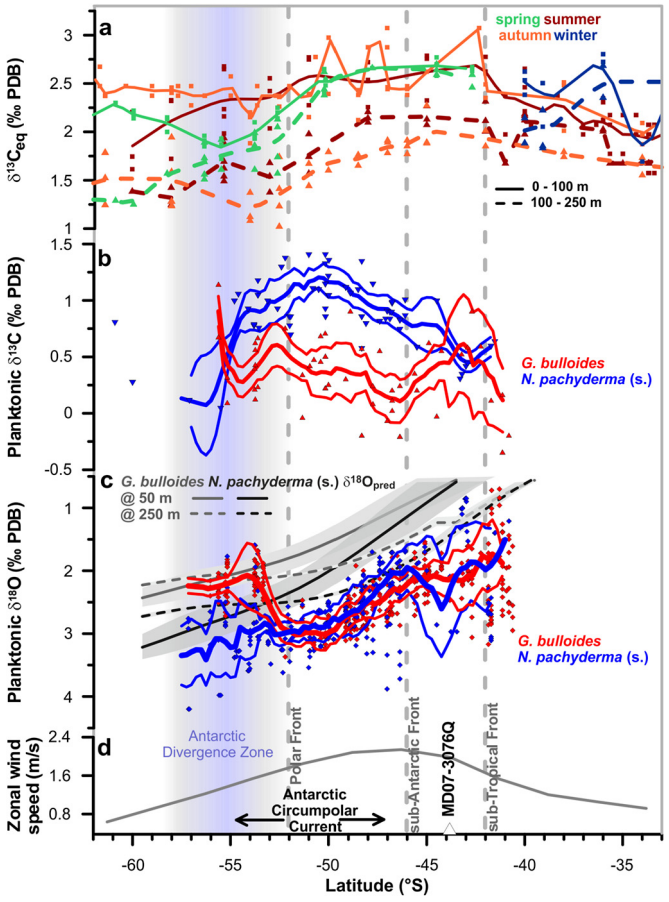

Fig. 3. South Atlantic latitudinal variations of a) equilibrium calcite $\delta^{13}C$ ($\delta^{13}C_{eq}$) inferred from surface water $\delta^{13}C$ of dissolved inorganic carbon (World Ocean Database 2009, Boyer et al., 2009; GLODAP database, Key et al., 2004; Mackensen et al., 1993) corrected for the Suess effect by $-0.018‰\,a^{-1}$ normalized to 1989 (the earliest measurement of the compiled data) (Gruber et al., 1999) shown for different seasons and water depths (0–100 m, squares; 100–250 m, triangles), b) stable carbon and c) oxygen isotopes of *G. bulloides* (red) and *N. pachyderma* (s.) (blue) obtained from core-top sediments (Hubberten and Niebler, unpubl.; Duplessy et al., 1991; Keigwin and Boyle, 1989; Kohfeld et al., 2000; Mulitza et al., 1997; Niebler, 1995; Niebler et al., 1999), red and blue lines indicate 2°-running averages (thick) and one sigma standard deviations (thin), grey shaded area and lines indicate seasonal and mean species-specific variations of predicted calcite $\delta^{18}O$ ($\delta^{18}O_{pred}$) calculated after Bemis et al. (1998) (13-chambered *G. bulloides*) and Mulitza et al. (2003) (*N. pachyderma* s.) for different water depths, d) the zonal annual wind stress obtained from the COADS climatology at 20°W (Woodruff et al., 1987); dashed grey lines and the triangle approximate the modern positions of the fronts (Orsi et al., 1995; Sokolov and Rintoul, 2009) and the core location, respectively. (For interpretation of the references to color in this figure legend, the reader is referred to the web version of this article.)

(Spero et al., 1997), changing $\delta^{13}C$ of *G. bulloides* by 0.013‰ per µmol kg^{-1} change in CO_3^{2-} concentration. Further, every 1‰ change in dietary $\delta^{13}C$ of particulate organic matter leads to the depletion of planktonic $\delta^{13}C$ by 0.084‰ (Spero and Lea, 1996). Dietary $\delta^{13}C$ variations as well as encrustation effects have been suggested to have a negligible impact on planktonic $\delta^{13}C$ (Kohfeld et al., 1996, 2000).

As shown in Fig. 4, we correct planktonic foraminifer $\delta^{13}C$ for these effects following Kohfeld et al. (2000), using temperatures for the assumed calcifying seasons and depth habitats of *G. bulloides* and *N. pachyderma* (s.) (WOA 2009, Locarnini et al., 2010), applying modern, mean annual CO_3^{2-} concentrations for the different planktonic depth habitats (GLODAP database, Key et al., 2004) and approximating dietary $\delta^{13}C$ by $\delta^{13}C$ of particulate organic matter (Goericke and Fry, 1994) (further details are given in the SOM). The resulting corrected planktonic $\delta^{13}C$ matches calcite $\delta^{13}C_{eq}$ derived

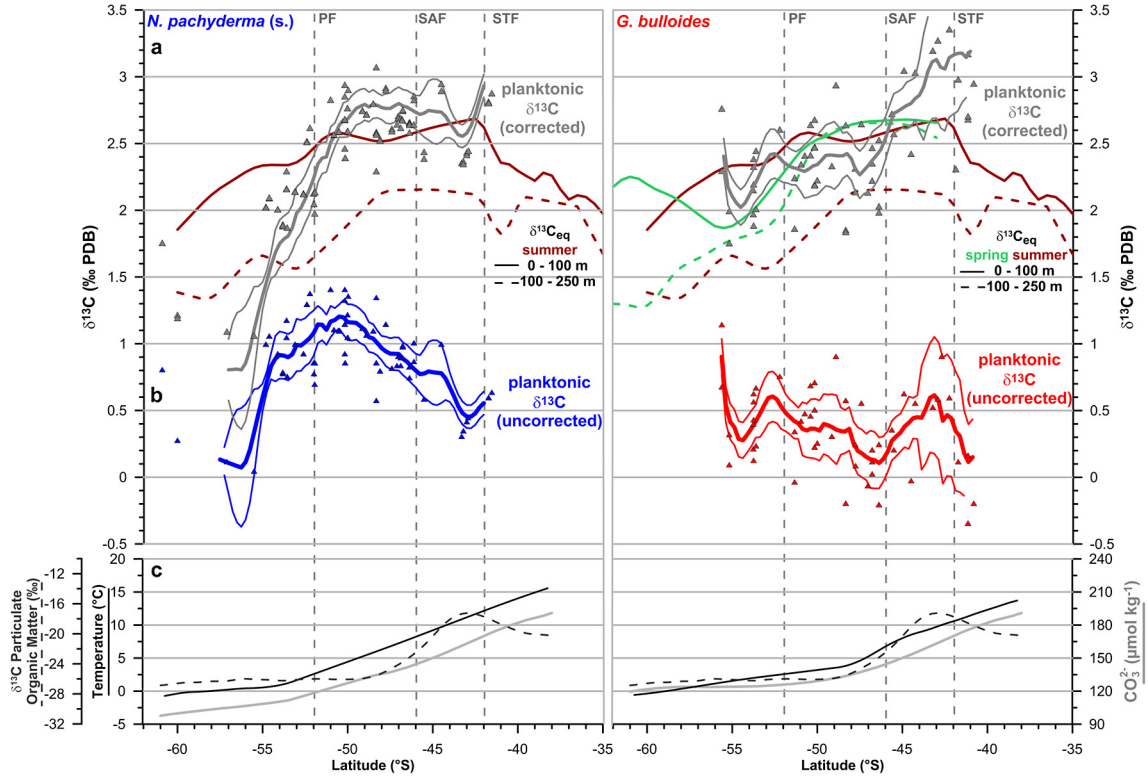

Fig. 4. Corrections of *N. pachyderma* (s.) (left) and *G. bulloides* (right) δ^{13}C: a) planktonic δ^{13}C corrected for the carbonate ion (CO_3^{2-})-, temperature- and dietary effect following Kohfeld et al. (2000) in comparison to seasonal equilibrium calcite δ^{13}C ($\delta^{13}C_{eq}$, 2°-running averages shown only) inferred from surface water δ^{13}C of dissolved inorganic carbon δ^{13}DIC ($\delta^{13}C_{eq} = \delta^{13}DIC + 1‰$; Romanek et al., 1992) in the expected season and habitat for each planktonic foraminifer (World Ocean Database 2009, Boyer et al., 2009; GLODAP database, Key et al., 2004; Mackensen et al., 1993), b) uncorrected core-top δ^{13}C of *N. pachyderma* (s.) (left) and *G. bulloides* (right) in the South Atlantic (thick and thin lines respectively indicate 2°-running averages and one sigma standard deviations), c) CO_3^{2-} concentrations along 20°W (GLODAP database, Key et al., 2004), modern surface water δ^{13}C of particulate organic matter as approximation of dietary δ^{13}C (Goericke and Fry, 1994) and ocean temperature along 20°W (World Ocean Atlas 2009, Locarnini et al., 2010) for the preferred habitats of both planktonic species used for the correction of planktonic δ^{13}C as outlined in the supporting online material; grey stippled lines indicate the approximate positions of the major fronts (PF – Polar Front, SAF – sub-Antarctic Front; STF – sub-Tropical Front).

from modern (1989) surface water δ^{13}DIC in the expected season and habitat of each planktonic species (Fig. 4). North of the PF, corrected *G. bulloides* and *N. pachyderma* (s.) δ^{13}C respectively match spring and summer equilibrium calcite δ^{13}C, whereas south of the PF corrected δ^{13}C of *N. pachyderma* (s.) coincides with calcite $\delta^{13}C_{eq}$ of much deeper water levels than corrected δ^{13}C of *G. bulloides* (Fig. 4). The general agreement of corrected planktonic δ^{13}C with expected calcite $\delta^{13}C_{eq}$ supports our assumptions on the preferred seasonal depth habitat of *G. bulloides* and *N. pachyderma* (s.) in the present-day Atlantic Sector of the Southern Ocean and points at the consistency of habitat affinities across the Southern Ocean today.

In summary, δ^{18}O- and δ^{13}C gradients between *G. bulloides* and *N. pachyderma* (s.) should faithfully record seasonal hydrographic changes of the upper water column north of the PF, with *G. bulloides* reflecting spring and *N. pachyderma* (s.) representing summer conditions, as well as the temperature-, salinity- and nutrient structure of the upper water column during summer south of the PF, given the following assumptions hold true: i) each foraminifer's broad habitat preference and dominant geochemical controls have not changed greatly over time, and ii) the seasonality and depth habitat of planktonic foraminifera south of Tasmania and in the sub-Antarctic Atlantic region are similar.

4.2. Planktonic δ^{18}O and δ^{13}C during the last deglaciation and MIS 3

During periods of rising $CO_{2,atm}$ during the last deglacial and glacial periods, δ^{18}O and δ^{13}C of *G. bulloides* and *N. pachyderma* (s.) diverge by up to 0.6‰ and 1‰, respectively (Fig. 5). *G. bulloides* δ^{18}O and δ^{13}C decrease, whereas *N. pachyderma* (s.) values tend to increase. δ^{18}O and δ^{13}C of both planktonic species converge during falling $CO_{2,atm}$ concentrations during the last deglaciation and MIS 3 (Fig. 5). Overall, planktonic $\Delta\delta^{13}$C co-varies with the rate of change in $CO_{2,atm}$ (Fig. 5), with one exception: during the $CO_{2,atm}$ rise associated with Antarctic warming event (Antarctic Isotopic Maximum, AIM) 1, δ^{18}O and δ^{13}C in *G. bulloides* and *N. pachyderma* (s.) diverge strongly but in the opposite direction to what is seen during other increases in $CO_{2,atm}$ of the last 68 ka (Fig. 5).

After AIM 1, the δ^{18}O of both species begin to diverge more strongly, reaching an offset of 1.2‰ during the last glacial maximum (LGM; Fig. 5). In fact, δ^{18}O of *N. pachyderma* (s.) matches δ^{18}O values observed in the deep-dwelling species *G. inflata* during the LGM (not shown). The δ^{18}O of *G. bulloides* and *N. pachyderma* (s.) commence to converge again at the beginning of the last deglaciation (Fig. 5).

4.3. Foraminiferal assemblage changes

Modern assemblages indicate the dominance of the sub-Antarctic species *G. bulloides* (50%) at the core location with minor contributions of the transitional species *G. inflata* (20%), the polar-water species *N. pachyderma* (s.) (20%) and the sub-Tropical species *N. pachyderma* (d.), *G. truncatulinoides* and *G. falconensis* (8%). This is in excellent agreement with the location of the study site within the present-day SAZ (Fig. 1). Prior to 18 ka BP, the polar species *N. pachyderma* (s.) dominated the sedimentary record up to 85%. This dominance is interrupted by short-term abundance decreases of *N. pachyderma* (s.) and the simultaneous increase in sub-Antarctic, transitional and sub-Tropical species (Fig. 6).

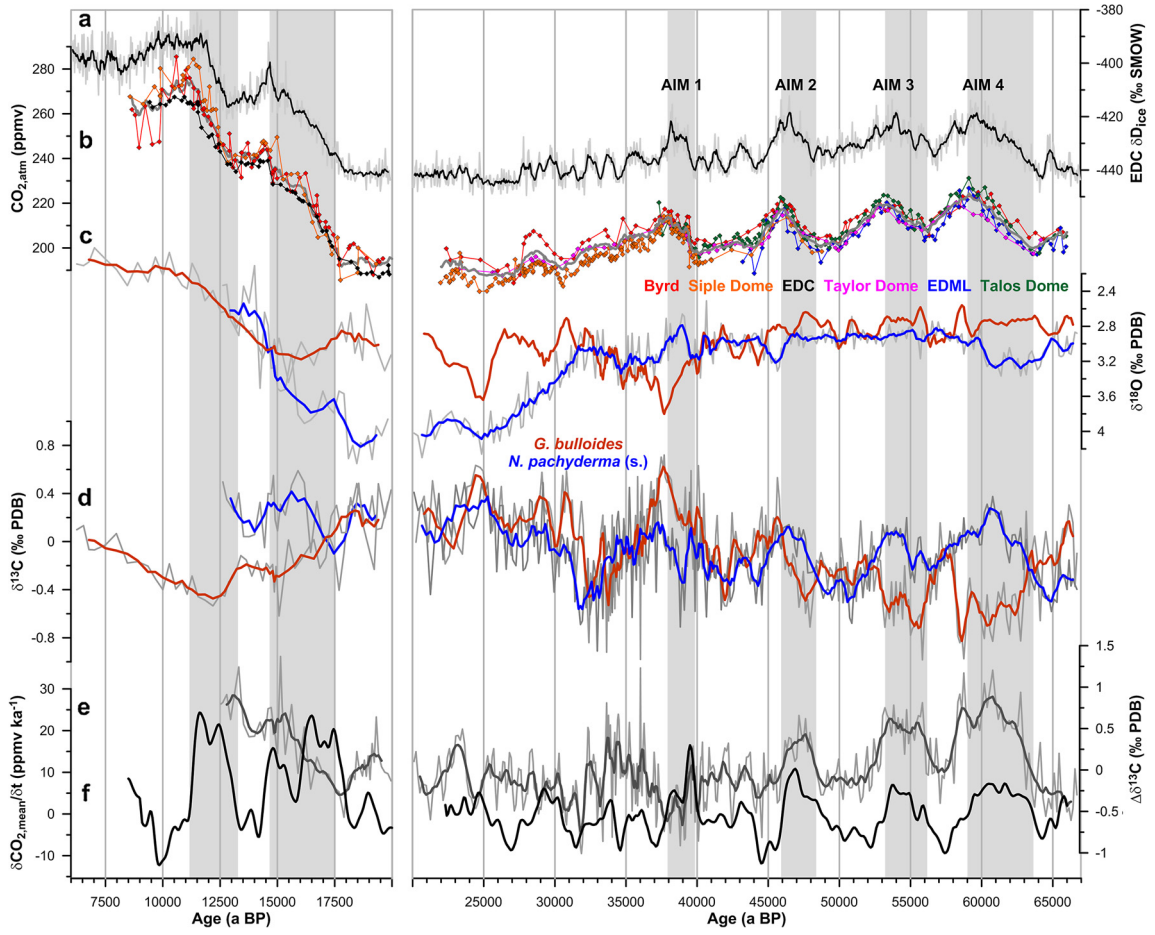

Fig. 5. a) δD record of the Antarctic ice core EPICA Dome C (EDC, Jouzel et al., 2007) transferred to the AICC2012 ice scale (Veres et al., 2013), b) variations in atmospheric CO_2 ($CO_{2,atm}$) observed in the Antarctic ice cores EPICA Dronning Maud Land (EDML, Bereiter et al., 2012; Lüthi et al., 2010), Talos Dome (Bereiter et al., 2012), Taylor Dome (Indermühle et al., 2000), Byrd (Ahn and Brook, 2008; Blunier and Brook, 2001), Siple Dome (Ahn and Brook, 2014; Ahn et al., 2004), Byrd (Neftel et al., 1988; Staffelbach et al., 1991) and EDC (Monnin et al., 2001) transferred to the AICC2012 age scale (Veres et al., 2013) as described in the supporting online material (mean in grey), c) δ^{18}O and d) δ^{13}C of *G. bulloides* (red, 5 pt-running average) and *N. pachyderma* (s.) (blue, 5 pt-running average), e) the corresponding $\Delta\delta^{13}$C (*N. pachyderma* (s.)–*G. bulloides*), f) the mean rate of $CO_{2,atm}$ change of the last deglaciation (left panel) and MIS 3 (right panel); grey bars indicate periods of rising $CO_{2,atm}$ levels. (For interpretation of the references to color in this figure legend, the reader is referred to the web version of this article.)

5. Discussion

5.1. Frontal shifts

Planktonic assemblages in sub-Antarctic sediment core MD07-3076Q mark millennial-scale variations in the dominance of Antarctic and sub-Antarctic surface waters at the core location. This implies the northward displacement of the PF and SAF as well as the expansion of Antarctic surface waters to the core site during the LGM and intervals of Antarctic cooling in MIS 3. In contrast, during periods of Antarctic warming in MIS 3 and the last deglaciation, planktonic assemblages suggest the preponderance of sub-Antarctic conditions resembling modern hydrographic conditions in the SAZ, which points at a southward retreat of the PF and SAF from the core site. The observed changes in planktonic assemblages are in agreement with results from a recent data compilation (Kohfeld et al., 2013) indicating a northward shift of oceanic fronts during (peak) glacial conditions.

5.2. Millennial-scale changes in sub-Antarctic Atlantic surface waters and $CO_{2,atm}$

5.2.1. Rises in $CO_{2,atm}$

A shift in the dominance from cold-water to sub-Antarctic and sub-Tropical species at the core site indicates the change from Antarctic to sub-Antarctic conditions during millennial-scale rises of $CO_{2,atm}$ during MIS 3 and the last deglaciation. Both δ^{18}O and δ^{13}C of *G. bulloides* and *N. pachyderma* (s.) show a marked divergence during these periods in contrast to intervals of low or decreasing $CO_{2,atm}$ levels, with the exception of AIM 1 (Fig. 5). Assuming the same seasonal habitat preferences of *G. bulloides* and *N. pachyderma* (s.) as in the modern SAZ (King and Howard, 2003, 2005), the negative excursions of δ^{13}C of *G. bulloides* during intervals of rising $CO_{2,atm}$ would document a marked depletion of surface water δ^{13}DIC during spring in comparison to today. This could be caused by stronger vertical mixing and enhanced upwelling of CO_2- and nutrient-enriched water to the surface ocean in winter and spring in the Antarctic Divergence Zone, leading to positive fluxes of CO_2 from the Southern Ocean to the atmosphere during this season and potentially contributing to net rises in $CO_{2,atm}$.

An alternative interpretation might be that a habitat shift to greater water depths could result in more depleted *G. bulloides* δ^{13}C (Fig. 3). However, this is relatively unlikely as such a deepening of the *G. bulloides* habitat is not observed in modern sediment trap or plankton tow studies anywhere in the Southern Ocean today and is also inconsistent with observed lighter *G. bulloides* δ^{18}O. Hence, we argue that winter-time upwelling of nutrients and concomitant decrease in density stratification of the upper water column cause the decrease in δ^{13}C of *G. bulloides*, which lends support to the hypothesized link of enhanced vertical mixing in

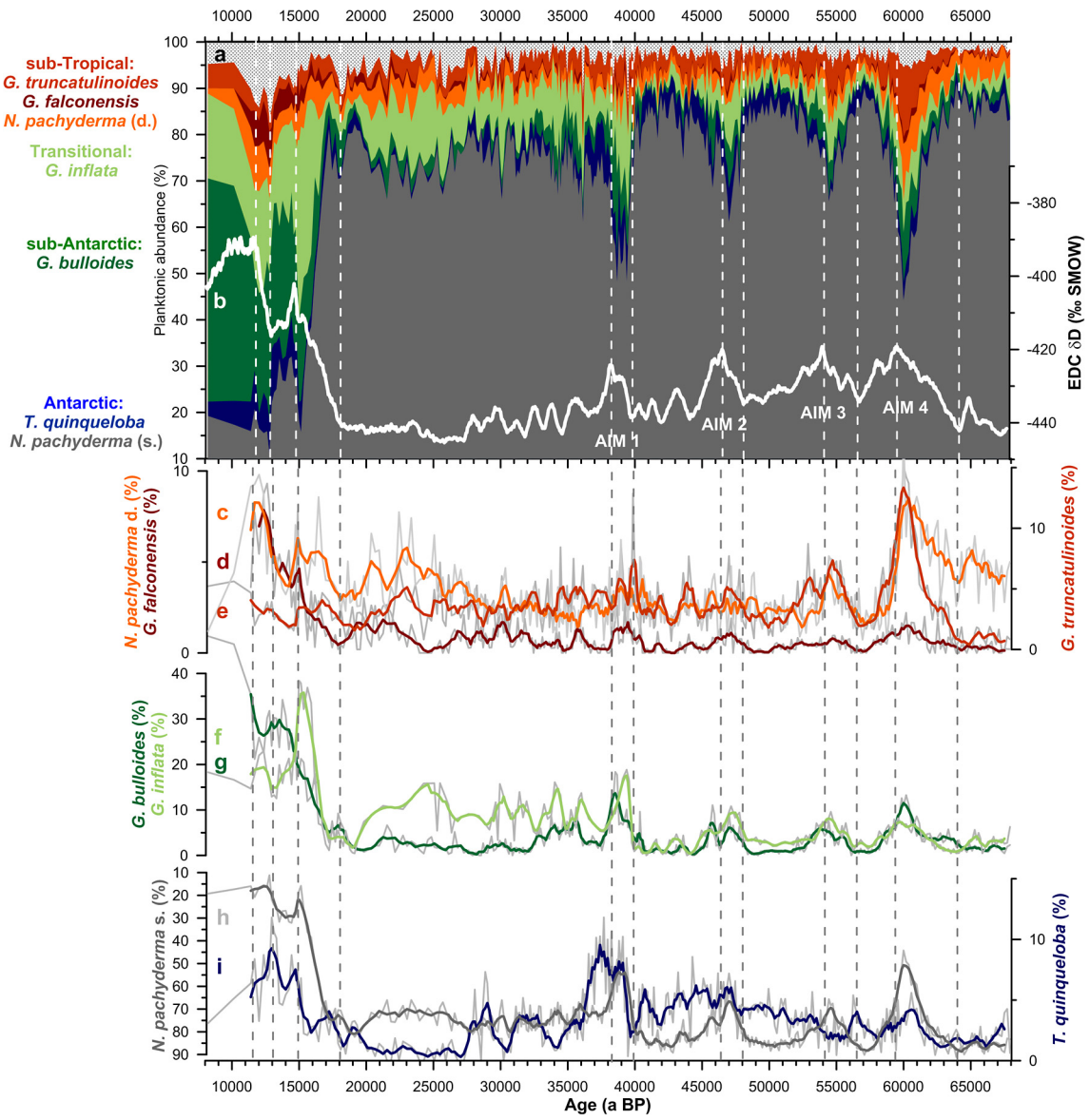

Fig. 6. Planktonic assemblage changes over the last 68 ka observed in MD07-3076Q: a) cumulative changes in planktonic foraminifer assemblages, b) the δD variability recorded in the EPICA Dome C (EDC) ice core (Jouzel et al., 2007) on the AICC2012 age scale (Veres et al., 2013), and relative changes in the abundance of c) *N. pachyderma* (d.), d) *G. falconensis*, e) *G. truncatulinoides*, f) *G. inflata*, g) *G. bulloides*, h) *N. pachyderma* (s.) and i) *T. quinqueloba*; dashed lines mark time intervals of warming in Antarctica.

the southern high-latitude ocean and millennial-scale $CO_{2,atm}$ rises during the last deglaciation and MIS 3 (e.g. Sachs and Anderson, 2005; Watson and Naveira Garabato, 2006).

These observations are consistent with deglacial planktonic $\delta^{13}C$ excursions observed in sediment cores from the Pacific and equatorial region (Siani et al., 2013; Spero and Lea, 2002). They further agree with millennial-scale changes in surface ocean stratification and associated vertical mixing in time with changes in $CO_{2,atm}$, which have been inferred from bulk sediment nitrogen isotope data in the sub-Antarctic Pacific (Robinson et al., 2007) and millennial-scale pulses in the export production of biogenic opal in the Southern Ocean south of the PF (Anderson et al., 2009).

While the $\delta^{13}C$ of *G. bulloides* decreases during millennial-scale rises in $CO_{2,atm}$, that of *N. pachyderma* (s.) increases (Fig. 5). We suggest that the rise in $\delta^{13}C$ of *N. pachyderma* (s.), which occupies a well-stratified water column during summer-time, reflects primarily an increase in export productivity (driving more complete nutrient depletion in summer) and secondarily an increase in air–sea gas exchange efficiency (driving the $\delta^{13}DIC$ of seawater to more positive values). Superficially, an increase in the export productivity in the central sub-Antarctic Atlantic might appear to be inconsistent with the proposed dust-driven reduction in nutrient utilization and therefore the export productivity observed in the Cape Basin in time with millennial-scale rises in $CO_{2,atm}$ (Martínez-García et al., 2009, 2014; Ziegler et al., 2013), and would also act against a proposed increase in the upwelling of nutrient-rich deep water with a high potential pCO_2 (Anderson et al., 2009) by tending to draw down $CO_{2,atm}$. However, these apparent conflicts may be resolved through the seasonal differentiation of these processes in the southern high-latitudes: increased upwelling and sub-surface nutrient supply as recorded by *G. bulloides* $\delta^{13}C$ in the sub-Antarctic Atlantic cause a depletion of surface water $\delta^{13}DIC$ and an enhanced nutrient availability primarily in spring, which would not necessarily influence *N. pachyderma* (s.) $\delta^{13}C$ during summer. Therefore, a lower nutrient utilization and decreased export production associated with reduced iron fertilization during intervals of rising $CO_{2,atm}$ inferred from decreases in *G. bulloides* $\delta^{15}N$ (Martínez-García et al., 2014) might occur during the spring season only, as we assume *G. bulloides* to predominantly thrive during the spring season (Section 4.1). Hence, strong gradients

between *G. bulloides* and *N. pachyderma* (s.) $\delta^{13}C$ might indicate the strong seasonal contrast of winter/spring-time upwelling of CO_2-rich water masses as well as the summer-time increase in nutrient utilization and biological export production in the surface ocean. The fact that these seasonally differentiated changes coincide with increasing multi-annual average $CO_{2,atm}$ would imply a dominant control of vertical mixing in the Southern Ocean and the related upwelling of CO_2-rich water masses during austral winter/spring on annually integrated Southern Ocean CO_2 fluxes and thus, on $CO_{2,atm}$ variations.

Above, we have interpreted the observed $\Delta\delta^{13}C$ between *G. bulloides* and *N. pachyderma* (s.) in terms of the primary controls on the δ^{13}DIC of seawater in the modern seasonal habitats of each species. Alternatively, these changes might be related to the processes that cause each foraminifer's isotopic signature to deviate from that of its ambient seawater (Section 4.1). However, we propose that such changes are unlikely to be the primary control of the observed $\Delta\delta^{13}C$ between *G. bulloides* and *N. pachyderma* (s.) during rises in $CO_{2,atm}$. An increased *N. pachyderma* (s.)–*G. bulloides* $\Delta\delta^{13}C$ gradient of about 1‰ translates into a spring to summer temperature gradient of 8 °C, or a CO_3^{2-} change of 100 µmol kg^{-1}, or a $\delta^{13}C_{org}$ change of 12‰. Considering the disequilibrium effects separately, SST, CO_3^{2-} concentrations and particulate organic matter $\delta^{13}C$ would have to vary by the whole range seen from 60°S to 30°S today from spring to summer (Fig. 4), and surface water temperatures in spring would have to be warmer than in summer to account for the observed changes in planktonic $\Delta\delta^{13}C$. These scenarios are rather unlikely. A combination of the various factors would also struggle to account for the full range of observed $\Delta\delta^{13}C$, as their effects on planktonic $\Delta\delta^{13}C$ partly work in opposite directions (Kohfeld et al., 2000).

Taken together, the observed variations in planktonic stable oxygen and carbon isotopes therefore suggest a significant impact on net annual marine CO_2 release due to enhanced vertical mixing in the southern high-latitude ocean during winter- and spring-time, as well as increased ocean–atmosphere CO_2 exchange throughout the remaining annual cycle. While enhanced nutrient supply from the sub-surface seems to have led to increased nutrient availability and enhanced CO_2 release during winter and spring, the opposite may have occurred in the summer, when nutrient availability was reduced. If the observed reduced nutrient availability translates into enhanced nutrient utilization and thus export production, the latter would imply that export productivity changes in the sub-Antarctic Atlantic in the summer did not exert a dominant control on $CO_{2,atm}$.

5.2.2. Antarctic warming event 1

During AIM 1, $\Delta\delta^{18}O$ and $\Delta\delta^{13}C$ of *G. bulloides* and *N. pachyderma* (s.) change sign, in contrast to what is observed during preceding periods of $CO_{2,atm}$ rise during MIS 3. This remains an enigma that we are unable to completely account for. One simple explanation would involve a swap of the calcifying seasons of *G. bulloides* and *N. pachyderma* (s.), which would be surprising as there is no analogue of this habitat change in the modern Southern Ocean. AIM 1 appears to be associated with a 'regime shift' in planktonic foraminifer assemblages and hydrographic conditions that probably reflects the transition into peak glacial conditions at the study site (Fig. 6). The approach of the sea ice margin to the core site during that time and the resulting influence of meltwater on the surface ocean density stratification, the nutrient budget and the air–sea CO_2 flux (Nelson and Smith, 1986; Sedwick and DiTullio, 1997) could in principle have led to 'no-modern-analogue' changes in the seasonality of *G. bulloides* and *N. pachyderma* (s.), and therefore the observed "anomalous" isotopic signatures.

5.2.3. LGM

The transition towards peak glacial conditions during the LGM is linked to an enrichment of *N. pachyderma* (s.) $\delta^{18}O$ in comparison to *G. bulloides* (Fig. 5), which indicates markedly different hydrographic conditions in the SAZ during the LGM compared to MIS 3. In fact, *N. pachyderma* (s.) $\delta^{18}O$ matches that of the thermocline-dweller *G. inflata*, which points at a habitat shift of *N. pachyderma* (s.). A strong $\delta^{18}O$ divergence between *G. bulloides* and *N. pachyderma* (s.) is observed in core-top samples from the sub-Antarctic Atlantic south of the PF today (Fig. 3). The strong $\delta^{18}O$ divergence of *G. bulloides* and *N. pachyderma* (s.) during the LGM thus implies the very strong influence of polar waters and an associated salinity-driven density stratification of the upper water column at the core site. A strong pycnocline therefore appears to have 'capped' the southern high-latitude ocean in summer during the LGM, at least as far north as the SAZ. This would have resulted in a year-round isolation of the sub-surface from the atmosphere, reducing the evasion of CO_2 to the atmosphere and leading to a drawdown of $CO_{2,atm}$ (e.g. François et al., 1997; Stephens and Keeling, 2000), consistent with evidence for expanded winter sea-ice and enhanced summer melt (Gersonde et al., 2003) as well as northward shifted westerlies (Toggweiler et al., 2006).

5.3. Comparison with planktonic records from the Cape Basin

Above, we have argued on the basis of the $\Delta\delta^{13}C$ between *G. bulloides* and *N. pachyderma* (s.) from the central sub-Antarctic Atlantic that enhanced vertical mixing in winter/spring and more effective air–sea CO_2 exchange in summer has a significant impact on millennial-scale $CO_{2,atm}$ variability. In order to test this proposition, we compare our data with planktonic stable isotope records from other sediment cores from the South Atlantic (locations are shown in Fig. 1): RC11-83 (Charles et al., 1996), TNO57-6 (Hodell et al., 2003), TNO57-10-11 (Hodell et al., 2000), and TNO57-21 (Mortyn et al., 2002). We smoothed the individual $\delta^{13}C$ records by a 1 ka-running average, detrended them by subtracting a 15 ka-running mean and calculated planktonic species-specific $\delta^{13}C$ stacks as mean of all available records (available from the Pangaea database).

To allow a direct comparison of the sediment records, we apply the most recent age scale for core TNO57-21 (Barker and Diz, 2014), which is based on the GICC05 age scale (Svensson et al., 2008) and which is equivalent to the Antarctic age scale AICC2012 (Veres et al., 2013) used in this study. Age control of RC11-83 prior to 41 ka is rather sparse, with only one tie point at the MIS4/3 boundary (Charles et al., 1996). We thus transferred the RC11-83 chronology on the GICC05 age scale (Svensson et al., 2008) based on the proposed chronostratigraphic alignment of benthic $\delta^{13}C$ of RC11-83 and TNO57-21 (Ninnemann and Charles, 2002; Piotrowski et al., 2008). The original radiocarbon-based age model is applied to the core section younger than 28 ka BP for RC11-83. The originally reported age models are used for sediment core TNO57-6 (Hodell et al., 2003) and TNO57-10-11 (Hodell et al., 2000).

The different planktonic $\delta^{13}C$ records exhibit common millennial-scale features, which points at a regional consistency of hydrographic changes in the sub-Antarctic Atlantic. Decreasing or minimum *G. bulloides* $\delta^{13}C$ values in RC11-83 and TNO57-21 coincide with intervals of rising $CO_{2,atm}$ during MIS 3 as observed in MD07-3076Q (Fig. 7). *G. bulloides* $\delta^{13}C$ in TNO57-6 generally follows the same trend and shows a $\delta^{13}C$ *G. bulloides* minimum during AIM 1. Peaks in *N. pachyderma* (s.) $\delta^{13}C$ observed in MD07-3076Q during rising $CO_{2,atm}$ are similar to those observed in TNO57-6, though the resolution is generally low. However, the *N. pachyderma* (s.) $\delta^{13}C$ record of RC11-83 strongly deviates from MD07-3076Q and close-by sediment cores TNO57-6 and

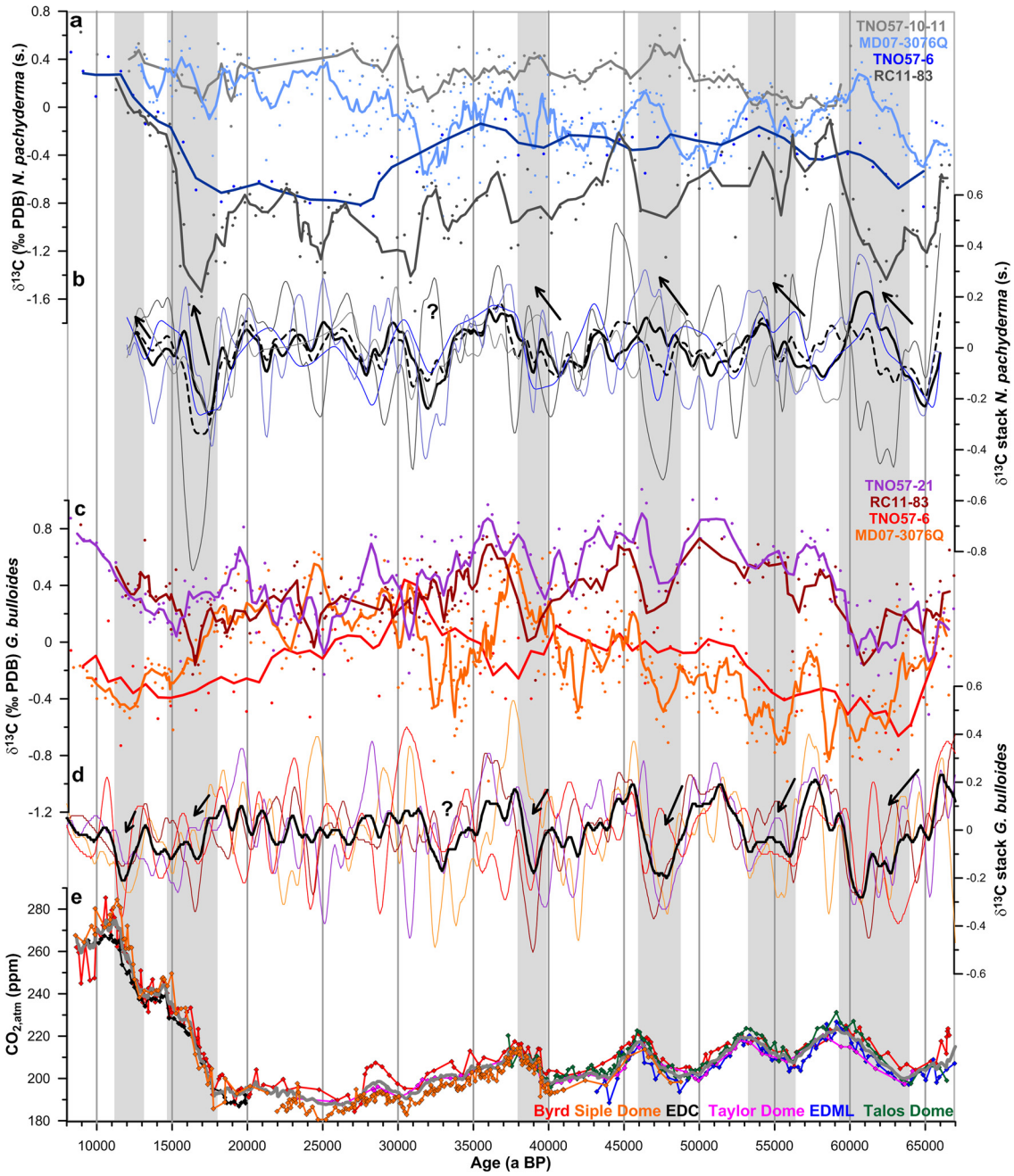

Fig. 7. Planktonic $\delta^{13}C$ records in the sub-Antarctic Atlantic: a) *N. pachyderma* (s.) $\delta^{13}C$ and c) *G. bulloides* $\delta^{13}C$ recorded in sediment core MD07-3076Q (solid line represents a 5-pt running average) and in sediment cores from the Cape Basin (RC11-83, Charles et al., 1996; TNO57-6, Hodell et al., 2003; TNO57-10-11, Hodell et al., 2000; TNO57-21, Mortyn et al., 2002; solid lines show 3-pt running averages); stack of smoothed (1 ka-running mean) and detrended records of b) *N. pachyderma* (s.) $\delta^{13}C$ (black solid and stippled line excludes and includes the RC11-83 record, respectively) and d) *G. bulloides* $\delta^{13}C$ (including all available records); e) changes in atmospheric CO_2 ($CO_{2,atm}$; references in Fig. 5); grey bars indicate periods of rising $CO_{2,atm}$ levels. (For interpretation of the references to color in this figure legend, the reader is referred to the web version of this article.)

TNO57-10-11, which may relate to inter-regional differences in the controls on planktonic $\delta^{13}C$ during summer, in particular in the Cape Basin. Overall, the stacked *G. bulloides* $\delta^{13}C$ values clearly decrease during intervals of increasing $CO_{2,atm}$, when the *N. pachyderma* (s.) $\delta^{13}C$ stack (omitting the "anomalous" RC11-83 *N. pachyderma* (s.) $\delta^{13}C$ record) generally shows marked increases (Fig. 7), which suggests that hydrographic changes inferred from proxy analyses in MD07-3076Q are not just localized phenomena, but may reflect basin-wide impacts. Moreover, a strong depletion in $\delta^{13}C$ of *G. bulloides* is observed during AIM 1 in RC11-83, TNO57-21 and TNO57-6, in contrast to MD07-3076Q (Section 5.2.3), suggesting that the "anomalous" observation in MD07-3076Q during AIM 1 is indeed a more localized phenomenon. These observations point at consistent hydrographic changes in the central and Southeast sub-Antarctic Atlantic during the last deglacial and glacial periods emphasizing the importance of seasonally differentiated impacts of the carbon cycling in the southern high-latitude ocean on $CO_{2,atm}$ over millennial time scales.

6. Summary

We present high-resolution $\delta^{18}O$ and $\delta^{13}C$ data from *G. bulloides* and *N. pachyderma* (s.) in conjunction with planktonic foraminifer census counts from the central sub-Antarctic Atlantic core MD07-3076Q, with accurate age control over the last deglacial

and glacial periods. Absolute chronologic uncertainties respectively amount to 1600 ± 500 years and to 1200 ± 400 years during MIS 3 and the last deglaciation, respectively.

By accounting for the CO_3^{2-}-, temperature- and dietary effects on planktonic carbon isotopes, we show that compiled core-top *G. bulloides* and *N. pachyderma* (s.) $\delta^{13}C$ data from the South Atlantic and the Atlantic Sector of the Southern Ocean are consistent with modern surface water $\delta^{13}DIC$ of the expected seasonal depth habitat of each foraminifer species. *G. bulloides* and *N. pachyderma* (s.) are thus interpreted to occupy (and record via their geochemistry) near-surface habitats in the SAZ during spring and summer, respectively (King and Howard, 2005, 2003). This provides a basis for reconstructing past changes in surface water $\delta^{13}DIC$ and its seasonal variability by means of planktonic stable isotopes.

Distinct decreases in *G. bulloides* $\delta^{13}C$ during intervals of rising $CO_{2,atm}$ indicate the depletion of surface water $\delta^{13}DIC$, and therefore enhanced upwelling of CO_2- and nutrient-rich water masses during winter and spring in the Antarctic Divergence Zone. Simultaneously, rising *N. pachyderma* (s.) $\delta^{13}C$ may indicate enhanced air–sea CO_2 exchange and/or reduced nutrient availability in summer. With the exception of *N. pachyderma* (s.) $\delta^{13}C$ in RC11-83, the observed patterns in planktonic isotopes in MD07-3076Q are consistent with available records from the Cape Basin, suggesting that they may be of basin-wide relevance. Enhanced upwelling of sub-surface CO_2-rich water during winter and spring, as well as enhanced air–sea exchange during summer, would thus have played a key role in driving past changes in surface ocean pCO_2 and therefore $CO_{2,atm}$ on millennial time scales.

Our data also suggest a marked difference in the hydrography of the Southern Ocean during the LGM, *versus* MIS 3 and the deglaciation. Following AIM 1, significantly enriched $\delta^{18}O$ values of *N. pachyderma* (s.) would indicate a deeper habitat of *N. pachyderma* (s.) in summer, in clear contrast to MIS 3 conditions. This could indicate a strong density stratification of the upper water column extending as far north as the SAZ during the LGM, perhaps associated with more extensive winter sea ice and a more intense summer melt season (Gersonde et al., 2003) as well as northward shifted westerlies (Toggweiler et al., 2006). This could have greatly diminished ocean–atmosphere CO_2 exchange and thus helped to draw $CO_{2,atm}$ levels down to their minimum LGM levels.

To sum up, in addition to underlining the important role that hydrographic changes in the Southern Ocean likely played in millennial-scale $CO_{2,atm}$ variability during the last deglaciation and MIS 3, our findings emphasize the significance of seasonally differentiated impacts of upwelling, air–sea gas exchange efficiency, surface ocean density stratification and export productivity on annually integrated fluxes of CO_2 from the Southern Ocean to the atmosphere and therefore changes in $CO_{2,atm}$. Our data suggest that during MIS 2 a year-round reduction in air–sea gas exchange due to a strong density stratification in the upper water column helped to drive $CO_{2,atm}$ concentrations to their minimum LGM levels, and that enhanced winter/spring upwelling has played a pivotal role in millennial-scale $CO_{2,atm}$ pulses during MIS 3 and the last deglaciation.

Acknowledgements

We are indebted to Fabien Dewilde, Gulay Isguder, James Rolfe and Ian Mather for preparing and performing isotopic analyses as well as Andreas Mackensen and Rainer Gersonde for sharing expertise in coring locations in the South Atlantic. We would like to thank Hans Hubberten, Hans-Stefan Niebler and Andreas Mackensen for sharing unpublished carbon isotope data from the South Atlantic. We thank two anonymous reviewers and the editor for their insightful comments and suggestions, which significantly helped to improve the manuscript. This work was supported by the Gates Cambridge Trust, the Royal Society and NERC grant NE/J010545/1. This is LSCE contribution 5366.

Appendix A. Supplementary material

Supplementary material related to this article can be found online at http://dx.doi.org/10.1016/j.epsl.2014.11.051. All data of this study are stored in the Pangaea database and are accessible via http://doi.pangaea.de/10.1594/PANGAEA.837069.

References

Ahn, J., Brook, E.J., 2008. Atmospheric CO_2 and climate on millennial time scales during the last glacial period. Science 322, 83–85. http://dx.doi.org/10.1126/science.1160832.

Ahn, J., Brook, E.J., 2014. Siple Dome ice reveals two modes of millennial CO_2 change during the last ice age. Nat. Commun. 5, 3723. http://dx.doi.org/10.1038/ncomms4723.

Ahn, J., Wahlen, M., Deck, B.L., Brook, E.J., Mayewski, P.A., Taylor, K.C., White, J.W.C., 2004. A record of atmospheric CO_2 during the last 40,000 years from the Siple Dome, Antarctica ice core. J. Geophys. Res., Atmos. 109. http://dx.doi.org/10.1029/2003JD004415.

Anderson, R.F., Ali, S., Bradtmiller, L.I., Nielsen, S.H.H., Fleisher, M.Q., Anderson, B.E., Burckle, L.H., 2009. Wind-driven upwelling in the Southern Ocean and the deglacial rise in atmospheric CO_2. Science 323, 1443–1448. http://dx.doi.org/10.1126/science.1167441.

Barker, S., Diz, P., 2014. Timing of the descent into the last ice age determined by the bipolar seesaw. Paleoceanography 29, 489–507. http://dx.doi.org/10.1002/2014PA002623.

Barker, S., Diz, P., Vautravers, M.J., Pike, J., Knorr, G., Hall, I.R., Broecker, W.S., 2009. Interhemispheric Atlantic seesaw response during the last deglaciation. Nature 457, 26. http://dx.doi.org/10.1038/nature07770.

Bé, A.W.H., 1969. Planktonic foraminifera. In: Antarctic Map Folio Series 11, pp. 9–12.

Belkin, I.M., Gordon, A.L., 1996. Southern Ocean fronts from the Greenwich meridian to Tasmania. J. Geophys. Res., Oceans 101, 3675–3696. http://dx.doi.org/10.1029/95JC02750.

Bemis, B.E., Spero, H.J., Bijma, J., Lea, D.W., 1998. Reevaluation of the oxygen isotopic composition of planktonic foraminifera: experimental results and revised paleotemperature equations. Paleoceanography 13, 150–160. http://dx.doi.org/10.1029/98PA00070.

Bemis, B.E., Spero, H.J., Lea, D.W., Bijma, J., 2000. Temperature influence on the carbon isotopic composition of *Globigerina bulloides* and *Orbulina universa* (planktonic foraminifera). Mar. Micropaleontol. 38, 213–228. http://dx.doi.org/10.1016/S0377-8398(00)00006-2.

Bereiter, B., Lüthi, D., Siegrist, M., Schüpbach, S., Stocker, T.F., Fischer, H., 2012. Mode change of millennial CO_2 variability during the last glacial cycle associated with a bipolar marine carbon seesaw. Proc. Natl. Acad. Sci. 109, 9755–9760. http://dx.doi.org/10.1073/pnas.1204069109.

Blunier, T., Brook, E.J., 2001. Timing of millennial-scale climate change in Antarctica and Greenland during the last glacial period. Science 291, 109. http://dx.doi.org/10.1126/science.291.5501.109.

Boyer, T.P., Antonov, J.I., Baranova, O.K., Garcia, H.E., Johnson, D.R., Locarnini, R.A., Mishonov, A.V., Seidov, D., Smolyar, I.V., Zweng, M.M., 2009. World Ocean Database 2009, Chapter 1: Introduction. In: Levitus, S. (Ed.), NOAA Atlas NESDIS 66. U.S. Government Printing Office, Washington, DC, pp. 1–216.

Charles, C.D., Lynch-Stieglitz, J., Ninnemann, U.S., Fairbanks, R.G., 1996. Climate connections between the hemisphere revealed by deep sea sediment core/ice core correlations. Earth Planet. Sci. Lett. 142, 19–27. http://dx.doi.org/10.1016/0012-821X(96)00083-0.

CLIMAP project members, 1984. The last interglacial ocean. Quat. Res. 21, 123–224. http://dx.doi.org/10.1016/0033-5894(84)90098-X.

Coplen, B., 1988. Normalization of oxygen and hydrogen isotope data. Chem. Geol. 12, 293–297. http://dx.doi.org/10.1016/0168-9622(88)90042-5.

Deuser, W.G., Ross, Eh., 1989. Seasonally abundant planktonic foraminifera of the Sargasso Sea; succession, deep-water fluxes, isotopic compositions, and paleoceanographic implications. J. Foraminiferal Res. 19, 268–293. http://dx.doi.org/10.2113/gsjfr.19.4.268.

Donner, B., Wefer, G., 1994. Flux and stable isotope composition of *Neogloboquadrina pachyderma* and other planktonic foraminifers in the Southern Ocean (Atlantic sector). Deep-Sea Res., Part 1, Oceanogr. Res. Pap. 41, 1733–1743. http://dx.doi.org/10.1016/0967-0637(94)90070-1.

Duplessy, J.C., Labeyrie, L., Juillet-Leclerc, A., Maitre, F., Duprat, J., Sarnthein, M., 1991. Surface salinity reconstruction of the North-Atlantic Ocean during the last glacial maximum. Oceanol. Acta 14, 311–324.

François, R., Altabet, M.A., Yu, E.F., Sigman, D.M., Bacon, M.P., Frank, M., Bohrmann, G., Bareille, G., Labeyrie, L.D., 1997. Contribution of Southern Ocean surface-water stratification to low atmospheric CO_2 concentrations during the last glacial period. Nature 389, 929–936. http://dx.doi.org/10.1038/40073.

Gebbie, G., Huybers, P., 2011. How is the ocean filled? Geophys. Res. Lett. 38, L6604. http://dx.doi.org/10.1029/2011GL046769.

Gersonde, R., Abelmann, A., Brathauer, U., Becquey, S., Bianchi, C., Cortese, G., Grobe, H., Kuhn, G., Niebler, H.-S., Segl, M., Sieger, M., Zielinski, U., Fütterer, D.K., 2003. Last glacial sea surface temperatures and sea-ice extent in the Southern Ocean (Atlantic–Indian sector): a multiproxy approach. Paleoceanography 18, 1–6. http://dx.doi.org/10.1029/2002PA000809.

Goericke, R., Fry, B., 1994. Variations of marine plankton $\delta^{13}C$ with latitude, temperature, and dissolved CO_2 in the world ocean. Glob. Biogeochem. Cycles 8, 85–90. http://dx.doi.org/10.1029/93GB03272.

Govin, A., Michel, E., Labeyrie, L., Waelbroeck, C., Dewilde, F., Jansen, E., 2009. Evidence for northward expansion of Antarctic Bottom Water mass in the Southern Ocean during the last glacial inception. Paleoceanography 24, 1202. http://dx.doi.org/10.1029/2008PA001603.

Gruber, N., Keeling, C.D., Bacastow, R.B., Guenther, P.R., Lueker, T.J., Wahlen, M., Meijer, H.A.J., Mook, W.G., Stocker, T.F., 1999. Spatiotemporal patterns of carbon-13 in the global surface oceans and the oceanic Suess effect. Glob. Biogeochem. Cycles 13, 307–335. http://dx.doi.org/10.1029/1999GB900019.

Haslett, J., Parnell, A., 2008. A simple monotone process with application to radiocarbon-dated depth chronologies. J. R. Stat. Soc. 57, 399–418. http://dx.doi.org/10.1111/j.1467-9876.2008.00623.x.

Hemleben, C., Spindler, M., Erson, O.R., 1989. Modern Planktonic Foraminifera. Springer, Berlin.

Hodell, D.A., Charles, C.D., Ninnemann, U.S., 2000. Comparison of interglacial stages in the South Atlantic sector of the southern ocean for the past 450 kyr: implications for Marine Isotope Stage (MIS) 11. Glob. Planet. Change 24, 7–26. http://dx.doi.org/10.1016/S0921-8181(99)00069-7.

Hodell, D.A., Venz, K.A., Charles, C.D., Ninnemann, U.S., 2003. Pleistocene vertical carbon isotope and carbonate gradients in the South Atlantic sector of the Southern Ocean. Geochem. Geophys. Geosyst. 4, 1–19. http://dx.doi.org/10.1029/2002GC000367.

Hughen, K., Southon, J., Lehman, S., Bertrand, C., Turnbull, J., 2006. Marine-derived ^{14}C calibration and activity record for the past 50,000 years updated from the Cariaco Basin. Quat. Sci. Rev. 25, 3216–3227. http://dx.doi.org/10.1016/j.quascirev.2006.03.014.

Indermühle, A., Monnin, E., Stauffer, B., Stocker, T.F., Wahlen, M., 2000. Atmospheric CO_2 concentration from 60 to 20 kyr BP from the Taylor Dome ice core, Antarctica. Geophys. Res. Lett. 27, 735–738. http://dx.doi.org/10.1029/1999GL010960.

Jonkers, L., Heuven, S., Zahn, R., Peeters, F.J.C., 2013. Seasonal patterns of shell flux, $\delta^{18}O$ and $\delta^{13}C$ of small and large *N. pachyderma* (s) and *G. bulloides* in the subpolar North Atlantic. Paleoceanography 28, 174–184. http://dx.doi.org/10.1002/palo.20018.

Jouzel, J., Masson-Delmotte, V., Cattani, O., Dreyfus, G., Falourd, S., Hoffmann, G., Minster, B., Nouet, J., Barnola, J.M., Chappellaz, J., Fischer, H., Gallet, J.C., Johnsen, S., Leuenberger, M., Loulergue, L., Luethi, D., Oerter, H., Parrenin, F., Raisbeck, G., Raynaud, D., Schilt, A., Schwander, J., Selmo, E., Souchez, R., Spahni, R., Stauffer, B., Steffensen, J.P., Stenni, B., Stocker, T.F., Tison, J.L., Werner, M., Wolff, E.W., 2007. Orbital and millennial Antarctic climate variability over the past 800,000 years. Science 317, 793. http://dx.doi.org/10.1126/science.1141038.

Keigwin, L.D., Boyle, E.A., 1989. Late Quaternary paleochemistry of high-latitude surface waters. Palaeogeogr. Palaeoclimatol. Palaeoecol. 73, 85–106. http://dx.doi.org/10.1016/0031-0182(89)90047-3.

Key, R.M., Kozyr, A., Sabine, C.L., Lee, K., Wanninkhof, R., Bullister, J.L., Feely, R.A., Millero, F.J., Mordy, C., Peng, T.-H., 2004. A global ocean carbon climatology: results from Global Data Analysis Project (GLODAP). Glob. Biogeochem. Cycles 18, GB4031. http://dx.doi.org/10.1029/2004GB002247.

King, A.L., Howard, W.R., 2003. Planktonic foraminiferal flux seasonality in Subantarctic sediment traps: a test for paleoclimate reconstructions. Paleoceanography 18, 1019. http://dx.doi.org/10.1029/2002PA000839.

King, A.L., Howard, W.R., 2005. $\delta^{18}O$ seasonality of planktonic foraminifera from Southern Ocean sediment traps: latitudinal gradients and implications for paleoclimate reconstructions. Mar. Micropaleontol. 56, 1–24. http://dx.doi.org/10.1016/j.marmicro.2005.02.008.

Kohfeld, K.E., Fairbanks, R.G., Smith, S.L., Walsh, I.D., 1996. *Neogloboquadrina pachyderma* (sinistral coiling) as paleoceanographic tracers in polar oceans: evidence from Northeast Water Polynya plankton tows, sediment traps, and surface sediments. Paleoceanography 11, 679–699. http://dx.doi.org/10.1029/96PA02617.

Kohfeld, K.E., Anderson, R.F., Lynch-Stieglitz, J., 2000. Carbon isotopic disequilibrium in polar planktonic foraminifera and its impact on modern and Last Glacial Maximum reconstructions. Paleoceanography 15, 53–64. http://dx.doi.org/10.1029/1999PA900049.

Kohfeld, K.E., Graham, R.M., de Boer, A.M., Sime, L.C., Wolff, E.W., Le Quéré, C., Bopp, L., 2013. Southern Hemisphere westerly wind changes during the Last Glacial Maximum: paleo-data synthesis. Quat. Sci. Rev. 68, 76–95. http://dx.doi.org/10.1016/j.quascirev.2013.01.017.

Kozdon, R., Ushikubo, T., Kita, N.T., Spicuzza, M., Valley, J.W., 2009. Intratest oxygen isotope variability in the planktonic foraminifer *N. pachyderma*: real vs. apparent vital effects by ion microprobe. Chem. Geol. 258, 327–337. http://dx.doi.org/10.1016/j.chemgeo.2008.10.032.

Kucera, M., Weinelt, M., Kiefer, T., Pflaumann, U., Hayes, A., Weinelt, M., Chen, M.-T., Mix, A.C., Barrows, T.T., Cortijo, E., Duprat, J., Juggins, S., Waelbroeck, C., 2005. Reconstruction of sea-surface temperatures from assemblages of planktonic foraminifera: multi-technique approach based on geographically constrained calibration data sets and its application to glacial Atlantic and Pacific Oceans. Quat. Sci. Rev. 24, 951–998. http://dx.doi.org/10.1016/j.quascirev.2004.07.014.

Locarnini, R.A., Mishonov, A.V., Antonov, J.I., Boyer, T.P., Garcia, H.E., Baranova, O.K., Zweng, M.M., Johnson, D.R., 2010. World Ocean Atlas 2009, vol. 1: Temperature. In: NOAA Atlas NESDIS 68. U.S. Government Printing Office, Washington, DC.

Lüthi, D., Bereiter, B., Stauffer, B., Winkler, R., Schwander, J., Kindler, P., Leuenberger, M., Kipfstuhl, S., Capron, E., Landais, A., Fischer, H., Stocker, T.F., 2010. CO_2 and O_2/N_2 variations in and just below the bubble-clathrate transformation zone of Antarctic ice cores. Earth Planet. Sci. Lett. 297, 226–233. http://dx.doi.org/10.1016/j.epsl.2010.06.023.

Lynch-Stieglitz, J., Stocker, T.F., Broecker, W.S., Fairbanks, R.G., 1995. The influence of air–sea exchange on the isotopic composition of oceanic carbon: observations and modeling. Glob. Biogeochem. Cycles 9, 653–665. http://dx.doi.org/10.1029/95GB02574.

Mackensen, A., Hubberten, H.-W., Bickert, T., Fischer, G., Fütterer, D.K., 1993. The $\delta^{13}C$ in benthic foraminiferal tests of Fontbotia wuellerstorfi (Schwager) relative to the $\delta^{13}C$ of dissolved inorganic carbon in southern ocean deep water: implications for glacial ocean circulation models. Paleoceanography 8, 587–610. http://dx.doi.org/10.1029/93PA01291.

Marinov, I., Gnanadesikan, A., Toggweiler, J.R., Sarmiento, J.L., 2006. The Southern Ocean biogeochemical divide. Nature 441, 964–967. http://dx.doi.org/10.1038/nature04883.

Marshall, J., Speer, K., 2012. Closure of the meridional overturning circulation through Southern Ocean upwelling. Nat. Geosci. 5, 171–180. http://dx.doi.org/10.1038/ngeo1391.

Martínez-García, A., Rosell-Melé, A., Geibert, W., Gersonde, R., Masqué, P., Gaspari, V., Barbante, C., 2009. Links between iron supply, marine productivity, sea surface temperature, and CO_2 over the last 1.1 Ma. Paleoceanography 24, PA1207. http://dx.doi.org/10.1029/2008PA001657.

Martínez-García, A., Sigman, D.M., Ren, H., Anderson, R.F., Straub, M., Hodell, D.A., Jaccard, S.L., Eglinton, T.I., Haug, G.H., 2014. Iron fertilization of the Subantarctic Ocean during the last ice age. Science 343, 1347–1350. http://dx.doi.org/10.1126/science.1246848.

Mashiotta, T.A., Lea, D.W., Spero, H.J., 1999. Glacial–interglacial changes in Subantarctic sea surface temperature and $\delta^{18}O$-water using foraminiferal Mg. Earth Planet. Sci. Lett. 170, 417–432. http://dx.doi.org/10.1016/S0012-821X(99)00116-8.

Metzl, N., Tilbrook, B., Poisson, A., 1999. The annual fCO_2 cycle and the air–sea CO_2 flux in the sub-Antarctic Ocean. Tellus B 51, 849–861. http://dx.doi.org/10.1034/j.1600-0889.1999.t01-3-00008.x.

Monnin, E., Indermühle, A., Dällenbach, A., Flückiger, J., Stauffer, B., Stocker, T.F., Raynaud, D., Barnola, J.M., 2001. Atmospheric CO_2 concentrations over the last glacial termination. Science 291, 112. http://dx.doi.org/10.1126/science.291.5501.112.

Mortyn, P.G., Charles, C.D., 2003. Planktonic foraminiferal depth habitat and $\delta^{18}O$ calibrations: plankton tow results from the Atlantic sector of the Southern Ocean. Paleoceanography 18, 1037. http://dx.doi.org/10.1029/2001PA000637.

Mortyn, P.G., Charles, C.D., Hodell, D.A., 2002. Southern Ocean upper water column structure over the last 140 kyr with emphasis on the glacial terminations. Glob. Planet. Change 34, 241–252. http://dx.doi.org/10.1016/S0921-8181(02)00118-2.

Mulitza, S., Dürkoop, A., Hale, W., Wefer, G., Niebler, H.S., 1997. Planktonic foraminifera as recorders of past surface–water stratification. Geology 25, 335–338. http://dx.doi.org/10.1130/0091-7613(1997)025<0335:PFAROP>2.3.CO;2.

Mulitza, S., Rühlemann, C., Bickert, T., Hale, W., Pätzold, J., Wefer, G., 1998. Late Quaternary $\delta^{13}C$ gradients and carbonate accumulation in the western equatorial Atlantic. Earth Planet. Sci. Lett. 155, 237–249. http://dx.doi.org/10.1016/S0012-821X(98)00012-0.

Mulitza, S., Boltovskoy, D., Donner, B., Meggers, H., Paul, A., Wefer, G., 2003. Temperature: $\delta^{18}O$ relationships of planktonic foraminifera collected from surface waters. Palaeogeogr. Palaeoclimatol. Palaeoecol. 202, 143–152. http://dx.doi.org/10.1016/S0031-0182(03)00633-3.

Neftel, A., Oeschger, H., Staffelbach, T., Stauffer, B., 1988. CO_2 record in the Byrd ice core 50,000–5,000 years bp. Nature 331, 609–611. http://dx.doi.org/10.1038/331609a0.

Nelson, D.M., Smith, W.O., 1986. Phytoplankton bloom dynamics of the western Ross Sea ice edge, II. Mesoscale cycling of nitrogen and silicon. Deep-Sea Res. 30, 1389–1412. http://dx.doi.org/10.1016/0198-0149(86)90042-7.

Niebler, H.-S., 1995. Reconstruction of paleo-environmental parameters using stable isotopes and faunal assemblages of planktonic foraminifera in the South Atlantic Ocean. Ber. Polarforsch. 167, 198.

Niebler, H.S., Gersonde, R., 1998. A planktic foraminiferal transfer function for the southern South Atlantic Ocean. Mar. Micropaleontol. 34, 213–234. http://dx.doi.org/10.1016/S0377-8398(98)00009-7.

Niebler, H.-S., Hubberten, H.-W., Gersonde, R., 1999. Oxygen isotope values of planktic foraminifera: a tool for the reconstruction of surface water stratification. In: Fischer, G., Wefer, G. (Eds.), Use of Proxies in Paleoceanography: Examples from the South Atlantic. Springer, pp. 165–189.

Ninnemann, U.S., Charles, C.D., 2002. Changes in the mode of Southern Ocean circulation over the last glacial cycle revealed by foraminiferal stable isotopic variability. Earth Planet. Sci. Lett. 201, 383–396. http://dx.doi.org/10.1016/S0012-821X(02)00708-2.

Nürnberg, D., Bijma, J., Hemleben, C., 1996. Assessing the reliability of magnesium in foraminiferal calcite as a proxy for water mass temperatures. Geochim. Cosmochim. Acta 60, 803–814. http://dx.doi.org/10.1016/0016-7037(95)00446-7.

Orsi, A.H., Whitworth, T., Nowlin, W.D., 1995. On the meridional extent and fronts of the Antarctic Circumpolar Current. Deep-Sea Res. 42, 641–673. http://dx.doi.org/10.1016/0967-0637(95)00021-W.

Peeters, F.J.C., Brummer, G.-J.A., Ganssen, G., 2002. The effect of upwelling on the distribution and stable isotope composition of *Globigerina bulloides* and *Globigerinoides ruber* (planktic foraminifera) in modern surface waters of the NW Arabian Sea. Glob. Planet. Change 34, 269–291. http://dx.doi.org/10.1016/S0921-8181(02)00120-0.

Peterson, R.G., Stramma, L., 1991. Upper-level circulation in the South Atlantic Ocean. Prog. Oceanogr. 26, 1–73. http://dx.doi.org/10.1016/0079-6611(91)90006-8.

Piotrowski, A.M., Goldstein, S.L., Hemming, S., Fairbanks, R.G., Zylberberg, D.R., 2008. Oscillating glacial northern and southern deep water formation from combined neodymium and carbon isotopes. Earth Planet. Sci. Lett. 272, 394–405. http://dx.doi.org/10.1016/j.epsl.2008.05.011.

Reimer, P.J., Baillie, M.G.L., Bard, E., Bayliss, A., Beck, J.W., Bertrand, C.J.H., Blackwell, P.G., Buck, C.E., Burr, G.S., Cutler, K.B., Damon, P.E., Edwards, R.L., Fairbanks, R.G., Friedrich, M., Guilderson, T.P., Hogg, A.G., Hughen, K.A., Kromer, B., McCormac, G., Manning, S., Ramsey, C.B., Reimer, R.W., Remmele, S., Southon, J.R., Stuiver, M., Talamo, S., Taylor, F.W., Plicht, J., van der Weyhenmeyer, C.E., 2004. INTCAL04 terrestrial radiocarbon age calibration, 0–26 cal kyr BP. Radiocarbon 46, 1029–1058.

Robinson, R.S., Mix, A., Martinez, P., 2007. Southern Ocean control on the extent of denitrification in the southeast Pacific over the last 70 ka. Quat. Sci. Rev. 26, 201–212. http://dx.doi.org/10.1016/j.quascirev.2006.08.005.

Romanek, C.S., Grossman, E.L., Morse, J.W., 1992. Carbon isotopic fractionation in synthetic aragonite and calcite: effects of temperature and precipitation rate. Geochim. Cosmochim. Acta 56, 419–430. http://dx.doi.org/10.1016/0016-7037(92)90142-6.

Sachs, J.P., Anderson, R.F., 2005. Increased productivity in the subantarctic ocean during Heinrich events. Nature 434, 1118–1121. http://dx.doi.org/10.1038/nature03544.

Sarmiento, J.L., Toggweiler, J.R., 1984. A new model for the role of the oceans in determining atmospheric pCO_2. Nature 308, 621–624. http://dx.doi.org/10.1038/308621a0.

Schmidt, G.A., Bigg, G.R., Rohling, E.J., 1999. Global Seawater Oxygen-18 Database — v1.21 [WWW Document]. http://data.giss.nasa.gov/o18data/.

Sedwick, P.N., DiTullio, G.R., 1997. Regulation of algal blooms in Antarctic shelf waters by the release of iron from melting sea ice. Geophys. Res. Lett. 24, 2515–2518. http://dx.doi.org/10.1029/97GL02596.

Siani, G., Michel, E., De Pol-Holz, R., DeVries, T., Lamy, F., Carel, M., Isguder, G., Dewilde, F., Lourantou, A., 2013. Carbon isotope records reveal precise timing of enhanced Southern Ocean upwelling during the last deglaciation. Nat. Commun. 4, 1–9. http://dx.doi.org/10.1038/ncomms3758.

Siegenthaler, U., Wenk, T., 1984. Rapid atmospheric CO_2 variations and ocean circulation. Nature 308, 624–626. http://dx.doi.org/10.1038/308624a0.

Sigman, D.M., Boyle, E.A., 2000. Glacial/interglacial variations in atmospheric carbon dioxide. Nature 407, 859–869. http://dx.doi.org/10.1038/35038000.

Sigman, D.M., Hain, M.P., Haug, G.H., 2010. The polar ocean and glacial cycles in atmospheric CO_2 concentration. Nature 466, 47–55. http://dx.doi.org/10.1038/nature09149.

Skinner, L.C., Fallon, S., Waelbroeck, C., Michel, E., Barker, S., 2010. Ventilation of the deep Southern Ocean and deglacial CO_2 rise. Science 328, 1147–1151. http://dx.doi.org/10.1126/science.1183627.

Skinner, L.C., Waelbroeck, C., Scrivner, A.E., Fallon, S.J., 2014. Radiocarbon evidence for alternating northern and southern sources of ventilation of the deep Atlantic carbon pool during the last deglaciation. Proc. Natl. Acad. Sci. 111, 5480–5484. http://dx.doi.org/10.1073/pnas.1400668111.

Sokolov, S., Rintoul, S.R., 2009. Circumpolar structure and distribution of the Antarctic Circumpolar Current fronts: 2. Variability and relationship to sea surface height. J. Geophys. Res., Oceans 114. http://dx.doi.org/10.1029/2008JC005108.

Spero, H.J., 1992. Do planktic foraminifera accurately record shifts in the carbon isotopic composition of seawater ΣCO_2? Mar. Micropaleontol. 19, 275–285. http://dx.doi.org/10.1016/0377-8398(92)90033-G.

Spero, H.J., Lea, D.W., 1996. Experimental determination of stable isotope variability in *Globigerina bulloides*: implications for paleoceanographic reconstructions. Mar. Micropaleontol. 28, 231–246. http://dx.doi.org/10.1016/0377-8398(96)00003-5.

Spero, H.J., Lea, D.W., 2002. The cause of carbon isotope minimum events on glacial terminations. Science 296, 522. http://dx.doi.org/10.1126/science.1069401.

Spero, H.J., Bijma, J., Lea, D.W., Bemis, B.E., 1997. Effect of seawater carbonate concentration on foraminiferal carbon and oxygen isotopes. Nature 390, 497–500. http://dx.doi.org/10.1038/37333.

Staffelbach, T., Stauffer, B., Sigg, A., Oeschger, H., 1991. CO_2 measurements from polar ice cores: more data from different sites. Tellus B 43, 91–96. http://dx.doi.org/10.1034/j.1600-0889.1991.t01-1-00003.x.

Stephens, B.B., Keeling, R.F., 2000. The influence of Antarctic sea ice on glacial–interglacial CO_2 variations. Nature 404, 171–174. http://dx.doi.org/10.1038/35004556.

Stramma, L., England, M., 1999. On the water masses and mean circulation of the South Atlantic Ocean. J. Geophys. Res. 104, 20863–20884. http://dx.doi.org/10.1029/1999JC900139.

Svensson, A., Andersen, K.K., Bigler, M., Clausen, H.B., Dahl-Jensen, D., Davies, S.M., Johnsen, S.J., Muscheler, R., Parrenin, F., Rasmussen, S.O., Röthlisberger, R., Seierstad, I., Steffensen, J.P., Vinther, B.M., 2008. A 60,000 year Greenland stratigraphic ice core chronology. Clim. Past 4, 47–57. http://dx.doi.org/10.5194/cp-4-47-2008.

Takahashi, T., Sutherland, S.C., Sweeney, C., Poisson, A., Metzl, N., Tilbrook, B., Bates, N., Wanninkhof, R., Feely, R.A., Sabine, C., Olafssong, J., Nojirih, Y., 2002. Global sea–air CO_2 flux based on climatological surface ocean pCO_2, and seasonal biological and temperature effects. Deep-Sea Res. 49, 1601–1622. http://dx.doi.org/10.1016/S0967-0645(02)00003-6.

Toggweiler, J.R., Russell, J.L., Carson, S.R., 2006. Midlatitude westerlies, atmospheric CO_2, and climate change during the ice ages. Paleoceanography 21, 2005. http://dx.doi.org/10.1029/2005PA001154.

Veres, D., Bazin, L., Landais, A., Kele, H.T.M., Lemieux-Dudon, B., Parrenin, F., Martinerie, P., Blayo, E., Blunier, T., Capron, E., Chappellaz, J., Rasmussen, S.O., Severi, M., Svensson, A., Vinther, B.M., Wolff, E., 2013. The Antarctic ice core chronology (AICC2012): an optimized multi-parameter and multi-site dating approach for the last 120 thousand years. Clim. Past 9, 1733–1748. http://dx.doi.org/10.5194/cpd-8-6011-2012.

Watson, A.J., Naveira Garabato, A.C., 2006. The role of Southern Ocean mixing and upwelling in glacial–interglacial atmospheric CO_2 change. Tellus B 58, 73–87. http://dx.doi.org/10.1111/j.1600-0889.2005.00167.x.

Weaver, P.P.E., Carter, L., Neil, H.L., 1998. Response of surface water masses and circulation to late Quaternary climate change east of New Zealand. Paleoceanography 13, 70–83. http://dx.doi.org/10.1029/97PA02982.

Williams, D.F., Bé, A.W.H., Fairbanks, R.G., 1981. Seasonal stable isotopic variations in living planktonic foraminifera from Bermuda plankton tows. Palaeogeogr. Palaeoclimatol. Palaeoecol. 33, 71–102. http://dx.doi.org/10.1016/0031-0182(81)90033-X.

Woodruff, S.D., Slutz, R.J., Jenne, R.L., Steurer, P.M., 1987. A comprehensive ocean–atmosphere data set. Bull. Am. Meteorol. Soc. 68, 1239–1250. http://dx.doi.org/10.1175/1520-0477(1987)068<1239:ACOADS>2.0.CO;2.

Wunsch, C., Ferrari, R., 2004. Vertical mixing, energy, and the general circulation of the oceans. Annu. Rev. Fluid Mech. 36, 281–314. http://dx.doi.org/10.1146/annurev.fluid.36.050802.122121.

Ziegler, M., Diz, P., Hall, I.R., Zahn, R., 2013. Millennial-scale changes in atmospheric CO_2 levels linked to the Southern Ocean carbon isotope gradient and dust flux. Nature 6, 457–461. http://dx.doi.org/10.1038/ngeo1782.